Manuscript

Title: Resident memory CD8$^+$ T cells in the upper respiratory tract prevent pulmonary influenza virus infection

Authors: Angela Pizzolla[1], Thi H.O. Nguyen[1], Jeffrey M Smith[1], Andrew G Brooks[1], Katherine Kedzieska[1], William R Heath[1], Patrick C Reading[1,3], Linda M Wakim[1] *

Affiliations:

[1]Department of Microbiology and Immunology, The University of Melbourne, at the Peter Doherty Institute for Infection and Immunity, Melbourne, Victoria 3000, Australia

[3] WHO Collaborating Centre for Reference and Research on Influenza, Victorian Infectious Diseases Reference Laboratory, at the Peter Doherty Institute for Infection and Immunity, Melbourne, Victoria 3000, Australia.

*Corresponding authors: LM Wakim (wakiml@unimelb.edu.au)

Running title: Influenza protective nasal resident memory CD8+ T cells

Abstract

Nasal epithelial tissue of the upper respiratory tract is the first site of contact by inhaled pathogens such as influenza virus. Here we show that this region is key to limiting viral spread to the lower respiratory tract and associated disease pathology. Immunization of the upper respiratory tract leads to the formation of local tissue-resident memory $CD8^+$ T cells (Trm). Unlike Trm in the lung, these cells develop independently of local cognate antigen recognition and TGFβ signaling and persist with minimal decay, representing a long-term protective population. Repertoire characterization revealed surprising differences between lung and nasal tissue Trm, the composition of which was shaped by the developmental need for lung, but not nasal tissue Trm, to recognize antigen within their local tissue. Importantly, we show that influenza-specific Trm in the nasal epithelia can block the transmission of influenza virus from the upper respiratory tract to the lung and in doing so prevent the development of severe pulmonary disease. Our findings reveal the protective capacity and longevity of upper respiratory tract Trm and highlight the potential of targeting these cells to augment protective responses induced to respiratory viral vaccines.

Introduction

Influenza is a highly contagious viral illness that continues to be a major public health burden, infecting 3-5 million people globally per annum. Human infections with seasonal influenza A viruses tend to be initiated and localized to the upper respiratory tract (URT) whereas pandemic and zoonotic viruses often cause severe disease, possibly due to increased tropism for the lower respiratory tract (LRT) (*1*). However, although seasonal influenza A virus infections are generally established in the upper airways, progression to the lung is essential for the development of viral pneumonia and severe disease (*2*). Although the URT represents an important site for initiation of infection and/or transmission of virus via coughing, sneezing or talking (*2*) little is currently known regarding the site-specific immunity present in the upper airways.

Much of what is known about the immune response following influenza virus infection of the respiratory tract has been deduced from studies of the lung (lower respiratory tract), because infections in this site are associated with more severe disease and increased risk of death. Protective immunity against influenza virus is tightly correlated with the persistence of influenza-specific tissue-resident memory $CD8^+$ T cells (Trm) in the lungs (*3*). Trm represent a memory T cell population that lodge in a variety of tissues (brain, intestine, female reproductive tract, salivary glands, lung, skin, liver) (*4-8*) and are marked by the expression of CD69 and in some cases CD103 (*9*). Although Trm in most tissues are long-lived and self-sustaining, Trm within the lung have been shown to require continued replenishment from a circulating effector memory T cell pool and gradually wane over time (*10*). Trm provide superior protection against local secondary infections through direct effector functions and by promoting the recruitment of circulating memory T cells. Recent work has implicated interleukin (IL)-15 and transforming growth factor (TGFβ□, as well as down-regulation of Krüppel-like Factor 2 (KLF2) (*11*), T-bet and eomes expression (*12*) and up-regulation of Hobit (*13*) in the formation and tissue retention of Trm. In addition to these universal Trm developmental requirements, local factors within the microenvironment in which these cells develop also influence their differentiation. Optimal development of influenza virus-specific $CD8^+$ Trm in the lung requires local antigen recognition, exposure to TGFβ and the presence of IFNγ-secreting $CD4^+$ T cells (*14-16*). Currently it is not

known if virus-specific $CD8^+$ Trm also develop in the URT, if their developmental requirements are similar to those of LRT Trm or whether they contribute to the control of influenza virus infection.

Herein we investigated the deposition, longevity and protective capacity of memory $CD8^+$ T cells in the URT following influenza virus infection. We show that influenza virus-specific Trm persisted long-term within the URT following intranasal influenza virus infection. We report that influenza specific Trm in the nasal epithelia can block the transmission of influenza virus from the URT to the lung and in doing so prevent the development of severe pulmonary disease. These results have substantial implications for intranasal vaccines that aim to elicit protective $CD8^+$ T-cell mediated immunity against respiratory pathogens and highlight the potential of URT Trm over lung Trm as key targets for respiratory viral vaccines.

Results

Influenza virus-specific memory CD8$^+$ T cells persist in the upper respiratory tract following virus infection

While influenza virus infection induces virus-specific CD8$^+$ Trm cells that persist in the lung parenchyma of mice (*3, 17, 18*), it was unclear whether CD8$^+$ Trm cells were also embedded in the upper respiratory tract. To formally assess whether influenza infection induces Trm at this site, congenically marked (CD45.1$^+$) OVA-specific OT-I TCR transgenic CD8$^+$ T cells were adoptively transferred into C57BL/6 recipients (CD45.2$^+$), which then received a total respiratory tract (TRT) infection with a recombinant influenza virus expressing the CD8 epitope from the model antigen OVA (X31-OVA). TRT infection (30 μl containing 10^4 PFU of virus delivered intranasally to anaesthetized mice) results in virus deposition and replication in both the lung (lower respiratory tract (LRT)) and nasal tissue (upper respiratory tract (URT)) (Fig 1a). Immunofluorescence analyses of the nasal tissue at day 6 post-infection revealed the presence of CD3$^+$ T cells in the nasal turbinates which congregated around cells which stained positive for influenza virus nucleoprotein (NP) (Fig 1b). The majority of OT-I T cells recovered from the lung and nasal tissue on day 35 p.i. showed elevated expression of CD103 and CD69, a phenotype used to identify Trm cells (Fig 1c). These CD103$^+$CD69$^+$ OT-I cells in the lung and nasal tissue appeared to emerge from a KLRG1-precursor population (Fig S1), which is consistent with previous reports that showed that skin Trm developed from effector CD8$^+$ T cells that lack KLRG1 expression (*19*). To validate that the CD103$^+$CD69$^+$ OT-I cells in the nasal tissue of the URT were 'bona fide' Trm we assessed whether they exhibited two key features of Trm, namely whether they were located within the nasal tissue parenchyma and persisted with minimal replenishment from the circulating memory CD8$^+$ T cell pool.

To determine the anatomical location of the CD103$^+$ OT-I cells in the nasal tissue we used an *in vivo* antibody labeling method to discriminate between CD8$^+$ T cells located within the circulation and the tissue. To do this, mice seeded with naïve OT-I T cells and receiving a TRT infection with X31-OVA 20 days earlier were injected intravenously (i.v.) with a fluorescently coupled anti-CD8 antibody 5 minutes prior to tissue harvest. The majority of OT-I T cells in the blood were stained with the i.v.-injected antibody, as did a proportion of OT-I cells within the spleen, confirming the efficiency of this *in vivo* labeling method (Fig 1d). Strikingly, few

$CD103^+$ OT-I cells in the nasal tissue and lung were labeled with the i.v.-injected antibody, reflecting that they were likely to be located outside the blood stream and lodged within the parenchyma tissue (Fig 1d).

We next assessed if the $CD103^+$ T cells in the nasal tissue persisted with minimal replenishment from the circulating population of memory $CD8^+$ T cells. To assess this, mice seeded with naïve OT-I.$CD45.1^+$ T cells and receiving TRT infection with X31-OVA 20 days earlier were administered a solution of carboxyfluorescein succinimidyl ester (CFSE) in a small volume via the i.n. route to limit labeling to cells of the URT. This technique labeled approximately 40% of $CD103^+$ OT-I in the nasal tissue as assessed 3 days after dye administration (Fig 1e-f). The proportion of $CFSE^+CD103^+$ OT-I T cells in the nasal tissue remained stable for a further 40 days post-dye administration, indicating that nasal tissue $CD103^+$ OT-I cells persist with minimal replenishment from the un-labeled circulating memory $CD8^+$ T-cell population and that turnover of the labeled cells was minimal.

We next assessed the distribution of $CD8^+$ Trm cells that develop within the nasal tissue following influenza virus infection. The nasal tissue of rodents contains nasal-associated lymphoid tissue (NALTs) which are mucosal-associated lymphoid organs embedded in the submucosa of the nasal passage (Fig 1g). NALTs consists of paired lymphoid tissue located at the base of the nasal cavities at the entrance of the nasopharyngeal duct and can be identified by microscopy of nasal tissue sections as densely packed clusters of B and T cells (Fig 1h). To determine the localization of influenza virus-specific Trm in the nasal tissue, mice injected with naïve OT-I.$CD45.1^+$ T cells received a TRT infection with X31-OVA and on day 20 p.i., mice were killed and nasal tissue sections prepared and stained to detect OT-I T cells (CD45.1+). In these sections, OT-I T cells were rare in NALTs but rather distributed throughout the nasal turbinate and septum (Fig 1i). To confirm these findings, NALTs were teased away from the palate of immune mice (generated as described above) and cellular composition was assessed by flow cytometry. OT-I.$CD45.1^+$ T cells were detected in both the NALTs and the nasal tissue (Fig 1j). Most OT-I T cells isolated from the NALTs and nasal tissue expressed CD103, although its MFI was consistently lower on OT-I T cells isolated from the NALTs (Fig 1k). Analysis of the distribution of $CD103^+$ OT-I Trm in the NALTs and nasal tissue revealed that the vast majority

of OT-I Trm following X31-OVA infection were localized outside the NALTs in the nasal tissue (Fig 1l).

Trm isolated from nasal tissue express Trm signature genes

To further authenticate that the $CD103^+CD69^+$ OT-I T cells persisting in the nasal tissue were Trm, their expression of a set of Trm core signature genes(*19, 20*) was assessed. Mice seeded with naïve OT-I cells received a TRT infection with X31-OVA and >30 days later subsets of OT-I memory T cells (identified based on expression of $CD103^+$ and $CD69^+$) were purified from nasal and lung tissues (Fig 2a). The expression of Trm signature genes in these cells was then compared with those expressed in splenic central ($CD62L^+$) and effector ($CD62L^-$) memory OT-I T cells isolated from the spleen of the same mice. Naïve OT-I T cells ($CD44^-$) were included as a control. As expected, genes defined as up-regulated in Trm (*Ctla4*, *Cdh1*, *Hsp1a*, *Itgae*, *Rgsl1*, *Skill*, *Xcl1)* were elevated in $CD103^+CD69^+$ OT-I cells isolated from both the lung and nasal tissue (Fig 2b, Fig S2). Likewise, genes down-regulated in Trm (*Eomes*, *Fam65b*, *S1p1r*, *Sidt1* and *Klf2)* were lower in $CD103^+CD69^+$ OT-I cells isolated from the lung and nasal tissue compared to the splenic memory T cell populations (Fig 2b, Fig S2). Collectively these results demonstrate that a population of $CD103^+CD69^+$ Trm persists within the nasal tissue of the URT following influenza virus infection.

Developmental requirements of Trm in the nasal tissue

Recent reports indicate that the optimal conversion of effector cytotoxic T lymphocytes into Trm cells within the lung requires both local antigen recognition and exposure to TGFβ (*3, 15, 21*). Therefore we next assessed whether Trm that develop in the nasal tissue of the URT were bound by the same differentiation requirements.

We assessed whether exposure to TGFβ facilitated Trm development in the nasal tissue of the URT. To do this, mice were seeded with either wild type naïve OT-I T cells or OT-I cells that lacked expression of the TGFβR (TGFβRII KO OT-I), then received a TRT infection with X31-OVA, and the infiltration of WT and TGFβRII KO OT-I cells into the lung and nasal tissue and their conversion into $CD103^+CD69^+$ Trm cells was assessed. There was little difference between the total number of WT and TGFβRII KO OT-I cells in the nose and lung at days 6-20 p.i. (Fig 2c-d), however the proportion of these cells that converted into Trm differed at each site (Fig 2e-

f). Consistent with previous reports, assessment of the number of $CD103^+$ $CD69^+$ OT-I cells that had elevated expression of the Trm markers CD103 and CD69 on day 60 revealed fewer TGFβR II KO OT-I cells compared with WT OT-I T cells expressed these markers in the lung up to day 60 p.i. (Fig 2e). However in the nasal tissue there was at best only a minor reduction (2.5-fold) in the number of TGFβR II KO OT-I cells expressing CD103 and CD69 compared with WT OT-I T cells (Fig 2f). To gain further insight into the identity of the $CD103^+CD69^+$ T cells that develop in nasal tissue independently of TGFβ signaling, these cells were assessed for the expression of key Trm signature genes. Critically, the majority of genes in our Trm signature panel (*Chd1, Itgae, Skil, Xcl1, Eomes, Fam65b, S1pr1, Sidt1* and *Klf2*) were all expressed in these $CD103^+CD69^+$ TGFβ□KO OT-I cells at similar levels to those observed in TGFβ sensitive $CD103^+CD69^+$ WT OT-I cells isolated from the nasal tissue (Fig 2g). The exception, *Ctla4*, was significantly elevated in the TGFβR II KO $CD103^+CD69^+$ OT-I cells compared to their WT equivalents, implicating a role for TGFβ as a regulator of expression of this gene. Although TGFβ exposure clearly boosts Trm cell differentiation in both the lung and nasal tissue following influenza virus infection, here we show that cells with a phenotypic and genetic Trm signature profile can develop in both these sites, albeit with varying efficiencies, independently of TGFβ signaling.

We next examined the requirement for local cognate antigen recognition in Trm cell differentiation in the URT. To do this, mice received a TRT infection with a parental strain of influenza virus (X31) or the strain that had been engineered to express the model antigen OVA (X31-OVA) 2 days before receiving 10^6 *in vitro*-activated effector OT-I $CD8^+$ T cells. Although effector OT-I T cells will be recruited to the lung and nasal tissue in both cohorts of mice, only in the group infected with the X31-OVA virus will interactions with local cognate antigen occur. The presence of $CD103^+CD69^+$ OT-I Trm in the respiratory tract was then assessed by flow cytometry day 20 p.i. in both cohorts of mice. As previously demonstrated, OT-I Trm only developed in the lung of mice that received X31-OVA infection, validating the requirement for local antigen recognition in lung Trm development (Fig 2h-i). In contrast, a similar proportion of OT-I converted into Trm in the nasal tissue of mice infected with either X31-OVA or X31 (Fig 2h). Hence the requirement for antigen in driving lodgment of Trm differed between the URT and the lung, with Trm being deposited in the nasal tissues via an "antigen-independent"

mechanism (Fig 2h-i). Nevertheless, the presence of local antigen within the nasal tissue did increase the number OT-I cells that converted into Trm which is consistent with recent reports that show local antigen also boosts the number of Trm that develop in the skin (*22*). Furthermore, local inflammation within the nose in response to influenza infection did increase the proportion of effector OT-I cells that converted into Trm, as in the absence of inflammation the conversion of the OT-I cells into nasal Trm was less efficient (Fig 2h), which is consistent with recent reports that show inflammatory environments favor Trm development (*10*).

Trm that develop in the URT persist with minimal decay and provide long term protection against influenza virus re-challenge

Trm that deposit within the murine lung following influenza virus infection undergo attrition, which limits their potential to provide long-term protection against future infections (*3*). We assessed if Trm lodged within the nasal tissue following influenza infection were also susceptible to the same numerical erosion. To compare the persistence of influenza virus-specific Trm in the nasal tissue and lung, mice injected with naïve OT-I T cells received a TRT infection with X31-OVA and the number of $CD103^{+}CD69^{+}$ OT-I Trm in these tissues 20, 60, 100 and 120 days later was measured. While the number of $CD103^{+}CD69^{+}$ OT-I Trm in the lung declined ~100-fold between day 20 and 120 p.i., strikingly, this population of cells remained relatively stable in the nasal tissue declining less than 2-fold over the same time period (Fig 3a).

We next determined if the persistence of Trm in the nasal tissue conferred prolonged local protection against secondary influenza virus infection. To assess this, mice seeded with naïve OT-I T cells and infected with a TRT X31-OVA infection were re-challenged 20 or 120 days later with a heterologous influenza virus which also expresses the CD8 epitope from the model antigen OVA (PR8-OVA). The use of a heterologous virus which expresses different HA and NA proteins to the primary strain allows the contribution of the humoral response to protection to be excluded. Viral growth in the nasal tissue and lung was determined 3 days later.
Consistent with prior reports (*3*), we observed that the capacity of influenza virus infected mice to control a secondary heterologous influenza virus infection of the lung waned over time. While mice re-challenged 20 days after the primary influenza infection exhibited a 20-fold reduction in

influenza viral titres in the lung (Fig 3b), mice re-challenged 120 days after the primary infection displayed minimal protection with viral titres in the lung tissue being comparable to that seen in a naïve cohort that only received the challenge virus. Strikingly, the protection against secondary heterologous influenza infection within the nasal tissue did not decay over the time course of this experiment. We observed significant reduction in viral titres in the nasal tissue of mice that were re-challenged at either 20 or 120 days after the primary infection (Fig 3c), which correlated with the stable persistence of influenza-specific Trm within the nasal tissue. The protective capacity and longevity of URT Trm mark these cells as ideal targets for respiratory viral vaccines.

Different immunodominance hierarchies among influenza-specific Trm in the lung and nasal tissue

We next assessed if we could achieve the same pattern of Trm lodgment along the respiratory tract when evoking an endogenous $CD8^+$ T cell response directed against influenza viral proteins. While viruses express many proteins, the virus-specific $CD8^+$ T cell responses generally segregate into reproducible hierarchies with certain epitopes eliciting either immunodominant or subdominant responses after virus infection. We tracked the influenza virus-specific $CD8^+$ T cell response against two classically defined immunodominant epitopes derived from the viral nucleoprotein (NP_{366}) and acid polymerase (PA_{224}) and a subdominate epitope derived from the viral polymerase ($PB1_{703}$) using H-$2D^b$ tetramers loaded with the PA_{224} and NP_{366} epitopes or H-$2K^b$ tetramers loaded with the $PB1_{703}$ epitope. Following a TRT infection with PR8, sizable populations of NP_{366}-, PA_{224}- and $PB1_{703}$- specific $CD8^+$ T cells could be detected in the spleen, lung and nasal tissue of mice at day 10 p.i. and while numbers contracted thereafter, long-term memory cells of all specificities were detectable in each of these sites at day 60 p.i. (Fig 4a-b). Consistent with prior reports (*21*, *23*)(*24*), splenic NP_{366}-specific $CD8^+$ T cells numerically dominated over PA_{224}- and $PB1_{703}$- specific $CD8^+$ T cells at day 10 p.i. however this effect was lost as cells progressed into long-term memory. Similarly, we observed the same pattern of immunodominance in the nasal tissue (Fig 4a-c), as previously reported (*24*). Of interest, we observed a different pattern of immunodominance in the lung where equivalent numbers of each of the three $CD8^+$ T cell specificities were recovered at the acute (day 10 p.i.) and late memory (day 60 p.i.) time points, although the numbers of each had dropped markedly by day 60 p.i. (Fig 4a-b).

To assess whether these influenza virus-specific $CD8^+$ T cells converted into Trm along the respiratory tract, mice receiving a TRT infection with PR8 were analysed at day 60 p.i. for the expression of Trm markers CD103 and CD69 by NP_{366}-, PA_{224}- and $PB1_{703}$- specific T cells recovered from the lung and nasal tissues. Strikingly, we observed that NP_{366}-, PA_{224}- and $PB1_{703}$- specific T cells differentiated into $CD103^+CD69^+$ Trm with different efficiencies depending on whether they developed into Trm within the lung or nasal tissue (Fig 4c-f). In the nasal tissue similar proportions (~55-65%) of NP_{366}-, PA_{224}- and $PB1_{703}$- specific T cells had up-regulated Trm markers at day 60 p.i (Fig 4d), and all three $CD8^+$ T cell specificities represented equivalent sized Trm populations at this site (Fig 4e). In the lung, ~60-70% of PA_{224}- and $PB1_{703}$- specific T cell pools had differentiated into $CD103^+CD69^+$ Trm by day 60 p.i. whereas the proportion of NP_{366}-specific T cells up-regulating these markers (~20%) was much lower (Fig 4d). The poor conversion of NP_{366}-specific T cells into Trm resulted in a significant reduction in the absolute number of NP_{366}-specific Trm cells in the lung compared to the other specificities (Fig 4f). Using the *in vivo* anti-CD8 labelling approach described earlier we confirmed that the reduction of $CD103^+CD69^+$ Trm NP_{366} -specific cells in the lung did correlate with a reduction of NP_{366} -specific cells within the lung parenchyma tissue as co-expression of these markers clearly identify cells localised to this compartment (Fig S3). Overall, we observed distinct immunodominace hierarchies within influenza virus specific Trm populations in the lung ($PB1_{703}$>PA_{224}>NP_{366}) compared to the nasal tissue ($PB1_{703}$=PA_{224}=NP_{366}) (Fig 4d-f). Collectively, these data show that the selection of different $CD8^+$ T cells specificities into the Trm pool is influenced by local factors within the microenvironment in which they develop.

Relative epitope abundance modulates the immunodominance hierarchy within the lung Trm pool

The development of Trm within the lung is heavily dependent on recognition of local cognate antigen. We speculated that changes in viral protein production, and thus epitope availability within the lung during virus infection might influence the immunodominance hierarchy and result in the preferential selection of different specificities into the Trm pool. To address this, mice primed by intraperitoneal (i.p.) infection with PR8 received bone marrow-derived dendritic cells (BMDCs) pulsed with equivalent doses of NP_{366}- and PA_{224}- peptide, or un-pulsed BMDCs

as control, (and adjuvant; LPS) 6 days later via the intranasal route. The development of NP_{366}- and PA_{224}- specific Trm cells in the lung was then determined 21 days after BMDC immunization (Fig 5a). In the spleens of control mice, (infected with PR8 via the i.p. route and given un-pulsed BMDCs), the numbers of NP_{366}-specific $CD8^+$ T cells exceeded the number of PA_{224}- specific $CD8^+$ T cells (Fig 5b), while in animals intranasally immunized with peptide-pulsed BMDCs the number of NP_{366}- and PA_{224}- specific $CD8^+$ T cells in the spleen were equivalent (Fig 5b). As expected, the proportions (Fig 5c) and numbers (Fig 5d) of NP_{366}-, or PA_{224}- specific $CD8^+$ Trm were negligible in the lungs of control animals, consistent with the requirement for local antigen recognition in lung Trm development (Fig 5c-d). In contrast, mice boosted by intranasal immunization with NP_{366}-/PA_{224}-peptide pulsed BMDCs or BMDC pulsed with the individual peptides (Fig S4) developed CD103+CD69+ Trm in the lung and delivery of equivalent doses of influenza virus epitopes resulted in equivalent proportions and numbers of NP_{366}- and PA_{224}-specific $CD8^+$ T cells developing into lung Trm (Fig 5c-d). These data indicate that the immunodominance hierarchy and selection of $CD8^+$ T cell specificities into the Trm pool within the lung may be a consequence of relative epitope abundance within the tissue over the course of the virus infection. In contrast, in the nasal tissue where there is no requirement for local cognate antigen recognition in Trm development all $CD8^+$ T cell specificities developed into Trm with equivalent efficiencies (Fig 4d-e).

Lodging influenza virus-specific Trm in the URT prevents pulmonary influenza virus disease.

In humans, influenza A virus infection is initiated and largely confined to the URT, although migration of the virus into the lungs can occur in high risk groups or with highly virulent influenza strains. Since the transmission of influenza virus from the URT to the lung is often associated with more severe disease, the capacity of Trm in the URT to prevent this transition was assessed. To do this, infection protocols that allow the selective deposition of Trm in either the upper (nose) or total respiratory tract (nose and lung) were established by exploiting the differential requirement for local antigen recognition in Trm development in these regions. The mouse-adapted PR8 strain of influenza virus does not disseminate efficiently from the upper (nasal tissue) to the lower (lung) respiratory tract (*25*). Therefore, when PR8 is administered as an URT infection (10 μl to the nares, no anesthetic) virus replication is largely localized to the

upper airways with limited replication in the lung (Fig 6a-b). In contrast, following TRT infection (30 μl to anesthetized mice), PR8 replicates in the nose and to high titres in the lung (Fig. 6a-b).

We addressed the impact of restricting influenza virus to the upper or total respiratory tract on Trm development within these compartments. Mice were infected either via the URT or TRT with PR8 and at day 30 p.i. the numbers of NP_{366}-, and PA_{224}-specific Trm in the lung and nasal tissue were determined, as well as the proportion of influenza tetramer+ cells in the spleen (as a reflection of the circulating memory T cell pool). Additionally, a control group of animals received an i.p. inoculation with PR8. As seen in Fig 6d, NP_{366}-, and PA_{224}-specific cells were observed in the spleens of all cohorts of mice. Animals that received PR8 by the i.p. route alone did not develop influenza-specific Trm in the lungs or nasal tissue (Fig 6 e-f). Following TRT infection, $CD103^+CD69^+$ NP_{366}-, and PA_{224}-specific Trm were detected in both the lung (Fig 6c,e) and nasal tissue (Fig 6c,f), however following URT infection tetramer+ Trm were only detected in nasal tissue (Fig 6c,e-f). Thus, we have developed an experimental model whereby influenza virus-specific Trm are lodged within the upper airways, but not in the lung.

We next determined if lodging influenza virus-specific Trm in the URT alone could prevent the development of pulmonary influenza virus infection. Mice infected as described above (URT, TRT or i.p. PR8), were rested for 30 days prior to a URT re-challenge with X31 (10 μl to the nares, no anesthetic), a heterologous virus strain capable of migrating into the lower respiratory tract following URT infection. At day 3 post-infection with X31, mice were killed and viral growth in the respiratory tract was determined. Compared to naïve mice that received a primary infection with X31, the presence of circulating memory T cells alone (i.p PR8 cohort) did not result in any significant reduction in viral titres in the nasal tissue (Fig 6g) or the lung (Fig 6h). In contrast, when the circulating memory T cell pool was supplemented by depositing influenza virus-specific $CD8^+$ Trm in the nasal tissue and lung (TRT PR8 cohort) virus growth in both the lung and nose was greatly reduced (Fig 6g-h). Strikingly, depositing Trm in the nasal tissue alone (URT PR8) was just as effective at reducing X31 growth in both the nose and the lung (Fig 6g-h). To confirm that deposition of Trm in the URT did not just delay the migration of the virus from the nasal tissue to the lung we repeated the above experiment but assayed the nasal tissue and lung 5 days after secondary X31 challenge. Again, we observed that deposition of Trm in the

nasal tissue alone (URT PR8) significantly reduced X31 growth in both the nose and the lung (Fig 6i-j). The depletion of all memory CD8 T cells from these PR8 primed mice (circulating and resident) prior to heterologous re-challenge with X31 abrogated the reduction in viral titres in the nasal tissue, validating that the control of influenza virus within this tissue was CD8+ T cell mediated (Fig S5). These data highlight the effectiveness of lodging Trm in the URT as an approach to limit the development of viral pneumonia in the lung.

Discussion

The respiratory tract is divided anatomically into upper (including the nose, mouth and pharynx) and lower (trachea, bronchi and lungs) compartments and is a major portal through which viruses enter the body. The URT represents an important site for initiation of infection and/or transmission of many human respiratory pathogens, including influenza virus. Despite this, little is known of the immunity that can be evoked within the URT. Therefore we investigated the deposition, protection and recall response of influenza virus-specific memory $CD8^+$ T cells in the URT. These studies showed that influenza virus-specific Trm developed within the URT following intranasal influenza virus infection. Moreover URT Trm rapidly cleared a secondary heterosubtypic influenza infection from the nasal mucosa and strikingly, in doing so, prevented virus spread into the lung. The upper respiratory tract is a key region to limiting viral spread to the lower respiratory tract and therefore in preventing the development of viral pneumonia and severe disease.

While virus-specific Trm lodge both within the URT and LRT following influenza virus infection, the differentiation requirements of Trm that develop in these compartments varied markedly. Nasal tissue (URT) Trm developed independently of local antigen recognition and were not heavily dependent on exposure to TGFβ for their differentiation. In contrast, optimal differentiation of lung Trm required both local antigen recognition (*3*) (*18*) and TGFβ signaling (*21*). The mechanism underlying the differences in Trm differentiation in the nasal tissue and lung remain unknown and while Trm development is most likely regulated by the tissue microenvironment and the local microbiota, we have yet to identify the factors that are essential for nasal tissue Trm development. Defining these conditions will be important to facilitate the development of vaccines that lodge Trm in the upper airways.

Although all the molecular factors that drive the differentiation and retention of Trm cells in their tissue of residency are not completely understood, TGFβ has been highlighted as one factor that facilitates Trm development in a variety of tissues. TGFβ signaling has been shown to induce the up-regulation of CD103 on Trm precursors and drives the down-regulation of t-box transcription factors Eomes and Tbet (*12*) – this series of events supports the deposition and retention of Trm in skin, gut and lung (*19, 21, 26, 27*). Although TGFβ exposure clearly improves Trm cell

differentiation in both the lung and nasal tissue following influenza virus infection, here we show that cells with a phenotypic and genetic Trm signature can develop in both these sites, albeit with varying efficiencies, independently of TGFβ signaling. In particular, the absence of TGFβ had minimal impact on the development and long-term persistence of Trm within the nasal tissue. While identifying the other environmental cues evoking Trm differentiation in the nasal tissue requires further investigation, potential candidates may include exposure to IL-15, tumor necrosis factor–α (TNFα) and IL-33(*11*) as all these cytokines have been implicated in Trm differentiation. This work further highlights the diversity among Trm that reside in different anatomical sites and emphasizes the local microenvironment as a key factor influencing the differentiation and maintenance of these cells.

While viruses express many proteins, virus-specific $CD8^+$ T cell responses are often directed at only a fraction of all the potential antigenic epitopes. The relative size of viral epitope-specific $CD8^+$ T cell responses generally segregate into reproducible hierarchies with certain epitopes eliciting either immunodominant or subdominant responses after virus infection. Earlier studies report that the immunodominance hierarchy of memory $CD8^+$ T cells recovered from the lung and nasal tissue after influenza infection mirrored the pattern observed within the circulating memory CD8 T cell compartment(*24, 28*). However, these studies profiled bulk influenza-specific memory CD8+ T cells within the upper and lower airways, which comprise a mixture of both Trm and circulating memory T cells. Here we show that the pattern of immunodominance observed among purified influenza virus-specific Trm isolated from the lung does not match the hierarchy observed within the circulating influenza virus-specific memory $CD8^+$ T cell compartment. More strikingly, we observed diversity within the immunodominance hierarchies among influenza virus-specific Trm pools located in the upper and lower respiratory tract.

Investigations on the efficiency in which different influenza-specific $CD8^+$ T cell specificities within a polyclonal response were recruited into the lung and nasal tissue Trm pool revealed striking differences in the immunodominance hierarchy at these sites. In the nasal tissue, NP_{366}-, PA_{224}- and $PB1_{703}$- specific $CD8^+$ T cells develop into Trm cells with equivalent efficiencies. As Trm development in the nasal tissue does not require local cognate antigen recognition all $CD8^+$ T cell specificities recruited to this site have an equal opportunity to develop into Trm as there is

no local selection process fine-tuning the repertoire. In contrast, in the lung, we observed that NP_{366}-, PA_{224}- and $PB1_{703}$- specific $CD8^+$ T cells adopted Trm status with varying efficiencies ranging from 20-70% Trm conversion. As Trm development in the lung is heavily dependent on local cognate antigen recognition, changes in viral protein production and epitope availability within the lung over the course of virus infection is likely to govern the selection of different specificities into the Trm pool. It is known that different influenza virus epitopes are presented by different cell types in the lung and this would likely result in a difference in the kinetics of antigen presentation of these epitopes over the course of virus infection (*29*). The tailoring of lung Trm diversity through antigen recognition is likely driven by a need for strict numeric limitations, given the sensitivity of this site to immunopathology. Our data supports recent findings that show antigen-dependent cross competition as a mechanism that shapes the repertoire of polyclonal antiviral Trm (*30*). Thus, antigen presentation within the tissue over the course of an infection is a factor that influences the recruitment of $CD8^+$ T cell specificities into the Trm pool, especially within microenvironments where Trm development is antigen dependent. Understanding what shapes the immunodominance hierarchy within these different memory $CD8^+$ T cell compartments and at these different anatomical locations is important, particularly with regards to developing vaccines that elicit effective memory $CD8^+$ T cell responses.

While mouse models and more recently clinical studies (*31*) confirm that Trm protect the lung from respiratory pathogens, this protection is only transient as Trm in the lung, unlike populations in the skin and intestinal mucosae, undergo attrition and decay in number, leaving the lung susceptible to re-infection (*3*). Slutter et al. recently reported that lung Trm are not self-sustaining and required continued replenishment from the circulating effector memory $CD8^+$ T cell pool in order to persist. The time-dependent loss of effector memory $CD8^+$ T cells from the circulating memory $CD8^+$ T cell compartment depleted the system of lung Trm precursor cells, and this was proposed to underlie the decay of lung Trm cells (*10*). The gradual loss of lung Trm may represent a mechanism to remove cells capable of evoking excessive inflammation and pathology from the lung, an organ noted for its intolerance for inflammation (*32*). While vaccination strategies that deposit influenza virus-specific Trm in the lung provide exquisite protection against heterosubtypic influenza challenge (*21*), the decay of lung Trm diminishes

their potential for long-term protection against future infections (*3*). Here we show that Trm in the nasal tissue of the URT are not susceptible to the same erosion and can provide long-term protection against secondary influenza virus infections. Trm present within the URT could also limit transmission of influenza virus from the upper to the lower airways. Hence, vaccination strategies that deposit Trm within the URT could safeguard the total respiratory tract and provide longer lasting protection against respiratory pathogens.

FluMist, the live attenuated influenza vaccine (LAIV) currently on the market is administered in the form of a nasal spray. Intranasal immunization with LAIV delivers the weakened influenza virus strains into the upper airways, and due to modifications which restrict replication to lower temperatures of the URT (<33^{o}C), this is where the virus remains (*33-35*). Though recent reports by Zens et al. (*36*) demonstrate that immunization of mice with LAIV results in highly protective humoral and cellular immune responses, as well as the development of lung Trm, the immunological outcomes of LAIV immunization in humans is ambiguous and likely impacted by differing levels of pre-existing influenza immunity between recipients (*37*). Immunization with LAIV does elicit robust influenza-specific neutralizing antibodies in humans and this response is initiated in the mucosal associated lymphoid tissue which service the upper airways (palatine tonsils) (*38*). However, the influenza-specific CD8^{+} T cell response evoked by the LAIV is highly variable (*39-41*).

Currently it is not known why the LAIV fails to elicit robust influenza specific CD8^{+} T cell responses. One possibility is that pre-existing humoral immunity in humans limits the replication of LAIV in the upper airways, providing sufficient antigen to boost B cell responses but insufficient for effective CD8^{+} T cell priming, expansion and/or activation. Moreover, the requirements for effective B cell priming/expansion may be anatomically distinct in the human airways to those for CD8^{+} T cells, such that only effective humoral responses are elicited. Defining CD8^{+} T cell priming, expansion, activation and decay in humans in response to LAIV is critical to uncover the immunological mechanisms underlying the apparent inability to induce effective CD8+ T cell (including Trm) immunity. While necessary, the design and execution of such studies in humans is extremely challenging. Greater understanding of the mechanisms involved in inducing effective cellular immunity and URT Trm development following

intranasal immunization will drive the development of effective new strategies that safeguard the upper airways from respiratory pathogens.

Our results demonstrate that heterosubtypic immunity to respiratory influenza challenge is tightly correlated with the presence of influenza virus-specific Trm within the respiratory tract. Our findings reveal the protective capacity and longevity of URT Trm and highlight the potential of these cells over lung T cells as key targets for respiratory viral vaccines.

Materials and Methods

Study design

The main aim of the study was to characterize the development of influenza virus specific resident memory T cells in the nasal tissue and assess the capacity of these cells to block influenza infection in the upper airways and stop the development of severe pulmonary disease. For this purpose, we adopted a mouse model of influenza virus infection and assessed nasal tissue resident memory T cell development using a model antigen system and transgenic OT-I CD8 T cells and complemented this work by tracking the endogenous CD8 T cell response.

All experiments were performed at least twice. The study involved sublethal infections with influenza A/Puerto Rico/8 (H1N1) PR8 or HongKong/31 (H3N2) X31 influenza viruses strains or these parental strains which were engineered by reverse genetics to express the model antigen Ovalbumin. No outliers were excluded from the data analyses.

Mice and viruses

C57BL/6, OT-I.CD45.1, *Tgfbr2*$^{f/f}$dLck-Cre OT-I.CD45.1 mice were bred in-house and housed in specific pathogen-free conditions in the animal facility at the Peter Doherty Institute of Infection and Immunity, the University of Melbourne, Melbourne, Australia. All experiments were done in accordance with the Institutional Animal Care and Use Committee guidelines of the University of Melbourne. Mice were infected intranasally with X31-OVA or PR8-OVA (*42*) (encodes the $OVA_{257–264}$ epitope within the neuraminidase stalk) generously provided by Dr. S. Turner, Monash University, Melbourne, Australia. For total respiratory tract infection (TRT) mice were anethestised with inhalation isofluorane anesthetic and infected with 50 PFU PR8 or PR8-OVA or 10^4 PFU of X31 or X31-OVA in a volume of 30 μl. For upper respiratory tract infection (URT) 10 μl of $10^{4.5}$ PFU of PR8, PR8-OVA or X31 virus was placed onto the nares of unanthestized mice.

In vivo labeling of T cells with CFSE or anti-CD8, and CD8 depletion

CFSE: 10 μl of 5mM CFSE diluted in RPMI were placed onto the nares of unanthestized mice.

Anti-CD8 antibody labeling: Mice were injected intravenously with 3 μg of phycoerythrin-conjugated antibody to CD8 (clone YTS-169) 5 min before they were killed. Mice were perfused

with PBS and tissues were collected, processed and stained with allophycocyanin-conjugated antibody to CD8 (anti-CD8; clone 53-6.7; eBioscience).

Anti-CD8 depletion: Mice were injected with 200 μg of anti-CD8 (clone 2.43, Walter & Eliza Hall Institute Antibody Facility) for 3 consecutive days or normal rat serum (NRS) and then every second day for the duration of the experiment.

Influenza virus plaque assay

Plaque assay for influenza virus was performed as described previously (*43*)

In vitro activation of OT-I cells

OT-I T cells were activated in vitro with 10^{-6} M SIINFEKL peptide pulsed splenocytes as previously described (*4*). Mice were injected with 10^6 *in vitro* activated effectors ($CD103^-CD69^-$).

Adoptive transfer and isolation of naïve T cells

Naïve OT-I CD8 T cells isolated from OT-I TCR transgenics mice were purified from single cell suspensions prepared from LN and spleen. Cells were purified after a depletion step using antibodies against CD11b (M1/70), F4/80, Ter-119, Gr-1 (RB6), MHC class II (M5/114), and CD4 (GK 1.5), followed by incubation with anti-rat IgG-coupled magnetic beads (Dynal Biotech) following the manufacturer's protocols. Naïve OT-I T cell preparations were 90–95% pure as determined by flow cytometry.

Bone marrow derived DC generation and immunization

Bone marrow flushed from tibias and femurs of C57BL/6 mice was resuspended at 1×10^6/mL in RPMI 1640 supplemented with 2.5 mM Hepes, 5.5 × 10−5 M mercaptoethanol, 100 U/mL penicillin, 100 μg/mL streptomycin, 5 mM glutamine, 10% FBS, and 10 ng/mL GM-CSF. Cells were incubated at 37 °C with 10% CO2 and cultured for 6 d with a media change on day 3. Dendritic cells were loaded with 10^{-6} M NP_{336} and PA_{224} peptide at 37 °C for 45 min. DCs were washed and re-suspended in 30 μl of PBS, and 2×10^6 cells with 1 μg of LPS was delivered intranasally into mice.

Isolation of nasal tissue and NALTs

The nasal tissue, including the nasal cavity, nasal turbinates and NALTs, were obtained by cutting down the vertical plane of the skull and scraping out the tissues and small bones from both sides of the nasal passages. The NALTs were extracted by removing the head from the body, dissecting away the lower jaw, tongue and connective tissue to expose the soft palate of the upper jaw. The front incisors were then cut away to reveal the anterior end of the soft palate. The palate was then peeled back from the anterior end, revealing the paired NALT structures at the posterior of the hard palate.

Flow cytometry and cell sorting

Single cell suspensions were prepared from spleens, LN and NALTs by mechanical disruption. Mice were perfused prior to the harvest of the lung tissue and nasal tissue which were enzymatically digested for 1 h at 37 °C in 3 mL of collagenase type 3 (3 mg/mL in RPMI 1640 supplemented with 2% FCS). Cells were stained for 25 min on ice with the appropriate mixture of monoclonal antibodies and washed with PBS with 1% BSA. The conjugated monoclonal antibodies were obtained from BD Pharmingen or eBioscience. H2-Db-NP_{366}, H2-Db-PA_{244} and H2-Kb-$PB1_{701}$ tetramers were made in house. Flow cytometry gating strategies are described in Fig S6 and Fig S7.

Real-time PCR

Cells were washed twice with PBS before RNA extraction by RNEasy Plus mini kit (Qiagen, Venlo, Netherlands). RNA template was prepared, at equal concentrations, and treated to in-solution DNAse I digestion (Sigma-Aldrich, St. Louis, USA) to remove trace genomic DNA (gDNA). Equal volumes of RNA template were used for each Sensifast cDNA synthesis reaction (Bioline, London, UK) prior to re-suspension of template in equal volumes of ultra-pure HPLC water. RT-PCR was performed with Sensifast Lo-ROX SYBR Green (Bioline, London, UK) on a MX3005P (Stratagene, La Jolla, USA) with a standardised 2ng of cDNA template used per well. Fold change was calculated relative to the geometric mean of 3 housekeeping genes (*RPL13a, HPRT, IPO8*).

Immunofluorescence microscopy

Euthanized mice were decapitated, their heads were skinned, and the lower jaws, including tongue, were removed. Tissue was fixed in 4 % paraformaldehyde for 6 hrs on ice, washed twice with PBS and incubated with agitation for 48hrs at room temperature in 20% EDTA. Tissue was embedded in OCT and frozen sections (14um) were cut using a cryostat. Tissue sections were acetone fixed, blocked in serum free protein block and stained with the specified antibodies from eBioscience, Biolegend or Abcam (CD3-Alexa660, CD45.1-Alexa647, B220-Alexa594, anti-influenza virus NP-FITC)

Statistical analysis

Comparison between two study groups was statistically evaluated by unpaired two tailed t test or Mann-Whitney test. Comparison between more than two groups (single factor) were evaluated using one-way analysis of variance (ANOVA) with Tukey's multiple comparison on log10 transformed values. Two way ANOVA with Sidak's multiple comparison on log10 transformed values was used to evaluate more than two groups at different time points. In all tests statistical significance was quantified as *P<0.5, **P<0.01, ***P<0.001 and ****P<0.0001. Statistical analysis was performed using GraphPad Prism 6 software.

Supplementary Materials

Fig S1. Lung and Nasal tissue Trm develop from KLRG1- precursor cells

Fig S2. Molecular signature of nasal tissue Trm

Fig S3. Localization of NP, PA and PB1 CD103+CD69+ Trm in the lung following post influenza virus infection

Fig S4. Trm development following DC immunization

Fig S5. Depletion of CD8 T cells eliminates local protection in the nasal tissue following influenza virus re-challenge

Fig S6. Gating strategy for identifying transgenic OT-I in spleen, lung and nasal tissue of influenza virus infected mice

Fig S7. Gating strategy for identifying endogenous influenza virus specific CD8+ T cells in spleen, lung and nasal tissue of influenza virus infected mice

Table S1 Source data file

References and Notes:

1. J. M. van den Brand *et al.*, Severity of pneumonia due to new H1N1 influenza virus in ferrets is intermediate between that due to seasonal H1N1 virus and highly pathogenic avian influenza H5N1 virus. *J Infect Dis* **201**, 993 (Apr 1, 2010).
2. J. Rello, A. Pop-Vicas, Clinical review: primary influenza viral pneumonia. *Crit Care* **13**, 235 (2009).
3. T. Wu *et al.*, Lung-resident memory CD8 T cells (TRM) are indispensable for optimal cross-protection against pulmonary virus infection. *J Leukoc Biol* **95**, 215 (Feb, 2014).
4. L. M. Wakim, A. Woodward-Davis, M. J. Bevan, Memory T cells persisting within the brain after local infection show functional adaptations to their tissue of residence. *Proc Natl Acad Sci U S A* **107**, 17872 (Oct 19, 2010).
5. T. Gebhardt *et al.*, Memory T cells in nonlymphoid tissue that provide enhanced local immunity during infection with herpes simplex virus. *Nat Immunol* **10**, 524 (May, 2009).
6. R. J. Hogan *et al.*, Protection from respiratory virus infections can be mediated by antigen-specific CD4(+) T cells that persist in the lungs. *J Exp Med* **193**, 981 (Apr 16, 2001).
7. D. Masopust *et al.*, Dynamic T cell migration program provides resident memory within intestinal epithelium. *J Exp Med* **207**, 553 (Mar 15, 2010).
8. D. Fernandez-Ruiz *et al.*, Liver-Resident Memory CD8+ T Cells Form a Front-Line Defense against Malaria Liver-Stage Infection. *Immunity* **45**, 889 (Oct 18, 2016).
9. S. N. Mueller, L. K. Mackay, Tissue-resident memory T cells: local specialists in immune defence. *Nat Rev Immunol* **16**, 79 (Feb, 2016).
10. B. Slutter *et al.*, Dynamics of influenza-induced lung resident memory T cells underlie waning heterosubtypic immunity. *Sci Immunol* **2**, (2017).
11. C. N. Skon *et al.*, Transcriptional downregulation of S1pr1 is required for the establishment of resident memory CD8+ T cells. *Nat Immunol* **14**, 1285 (Dec, 2013).
12. L. K. Mackay *et al.*, T-box Transcription Factors Combine with the Cytokines TGF-beta and IL-15 to Control Tissue-Resident Memory T Cell Fate. *Immunity* **43**, 1101 (Dec 15, 2015).
13. L. K. Mackay *et al.*, Hobit and Blimp1 instruct a universal transcriptional program of tissue residency in lymphocytes. *Science* **352**, 459 (Apr 22, 2016).
14. G. Infusini *et al.*, Respiratory DC Use IFITM3 to Avoid Direct Viral Infection and Safeguard Virus-Specific CD8+ T Cell Priming. *PloS one* **10**, e0143539 (2015).
15. D. L. Turner *et al.*, Lung niches for the generation and maintenance of tissue-resident memory T cells. *Mucosal Immunol*, (Sep 25, 2013).
16. B. J. Laidlaw *et al.*, CD4+ T cell help guides formation of CD103+ lung-resident memory CD8+ T cells during influenza viral infection. *Immunity* **41**, 633 (Oct 16, 2014).
17. K. G. Anderson *et al.*, Cutting edge: intravascular staining redefines lung CD8 T cell responses. *J Immunol* **189**, 2702 (Sep 15, 2012).
18. L. M. Wakim, N. Gupta, J. D. Mintern, J. A. Villadangos, Enhanced survival of lung tissue-resident memory CD8(+) T cells during infection with influenza virus due to selective expression of IFITM3. *Nat Immunol* **14**, 238 (Jan 27, 2013).
19. L. K. Mackay *et al.*, The developmental pathway for CD103CD8 tissue-resident memory T cells of skin. *Nat Immunol*, (Oct 27, 2013).
20. L. M. Wakim *et al.*, The molecular signature of tissue resident memory CD8 T cells isolated from the brain. *J Immunol* **189**, 3462 (Oct 1, 2012).

21. L. M. Wakim, J. Smith, I. Caminschi, M. H. Lahoud, J. A. Villadangos, Antibody-targeted vaccination to lung dendritic cells generates tissue-resident memory CD8 T cells that are highly protective against influenza virus infection. *Mucosal Immunol* **8**, 1060 (Sep, 2015).
22. T. N. Khan, J. L. Mooster, A. M. Kilgore, J. F. Osborn, J. C. Nolz, Local antigen in nonlymphoid tissue promotes resident memory CD8+ T cell formation during viral infection. *J Exp Med* **213**, 951 (May 30, 2016).
23. T. Cukalac *et al.*, Multiplexed combinatorial tetramer staining in a mouse model of virus infection. *J Immunol Methods* **360**, 157 (Aug 31, 2010).
24. J. A. Wiley, R. J. Hogan, D. L. Woodland, A. G. Harmsen, Antigen-specific CD8(+) T cells persist in the upper respiratory tract following influenza virus infection. *J Immunol* **167**, 3293 (Sep 15, 2001).
25. K. M. Edenborough, B. P. Gilbertson, L. E. Brown, A mouse model for the study of contact-dependent transmission of influenza A virus and the factors that govern transmissibility. *J Virol* **86**, 12544 (Dec, 2012).
26. B. S. Sheridan *et al.*, Oral infection drives a distinct population of intestinal resident memory CD8(+) T cells with enhanced protective function. *Immunity* **40**, 747 (May 15, 2014).
27. N. Zhang, M. J. Bevan, Transforming Growth Factor-beta Signaling Controls the Formation and Maintenance of Gut-Resident Memory T Cells by Regulating Migration and Retention. *Immunity* **39**, 687 (Oct 17, 2013).
28. G. T. Belz, W. Xie, J. D. Altman, P. C. Doherty, A previously unrecognized H-2D(b)-restricted peptide prominent in the primary influenza A virus-specific CD8(+) T-cell response is much less apparent following secondary challenge. *J Virol* **74**, 3486 (Apr, 2000).
29. S. R. Crowe *et al.*, Differential antigen presentation regulates the changing patterns of CD8+ T cell immunodominance in primary and secondary influenza virus infections. *J Exp Med* **198**, 399 (Aug 04, 2003).
30. A. Muschaweckh *et al.*, Antigen-dependent competition shapes the local repertoire of tissue-resident memory CD8+ T cells. *J Exp Med*, (Nov 29, 2016).
31. A. Jozwik *et al.*, RSV-specific airway resident memory CD8+ T cells and differential disease severity after experimental human infection. *Nat Commun* **6**, 10224 (Dec 21, 2015).
32. K. G. Anderson, D. Masopust, Editorial: Pulmonary resident memory CD8 T cells: here today, gone tomorrow. *J Leukoc Biol* **95**, 199 (Feb, 2014).
33. H. Jin *et al.*, Multiple amino acid residues confer temperature sensitivity to human influenza virus vaccine strains (FluMist) derived from cold-adapted A/Ann Arbor/6/60. *Virology* **306**, 18 (Feb 1, 2003).
34. Z. Wang *et al.*, Establishment of memory CD8+ T cells with live attenuated influenza virus (LAIV) across different vaccination doses. *J Gen Virol*, (Nov 02, 2016).
35. E. Hoffmann *et al.*, Multiple gene segments control the temperature sensitivity and attenuation phenotypes of ca B/Ann Arbor/1/66. *J Virol* **79**, 11014 (Sep, 2005).
36. K. D. Zens, J. K. Chen, D. L. Farber, Vaccine-generated lung tissue-resident memory T cells provide heterosubtypic protection to influenza infection. *JCI Insight* **1**, (Jul 07, 2016).

37. C. S. Ambrose, M. J. Levin, R. B. Belshe, The relative efficacy of trivalent live attenuated and inactivated influenza vaccines in children and adults. *Influenza Other Respir Viruses* **5**, 67 (Mar, 2011).
38. K. G. Mohn *et al.*, Live Attenuated Influenza Vaccine in Children Induces B-Cell Responses in Tonsils. *J Infect Dis* **214**, 722 (Sep 1, 2016).
39. P. A. Lanthier *et al.*, Live attenuated influenza vaccine (LAIV) impacts innate and adaptive immune responses. *Vaccine* **29**, 7849 (Oct 13, 2011).
40. X. S. He *et al.*, Phenotypic changes in influenza-specific CD8+ T cells after immunization of children and adults with influenza vaccines. *J Infect Dis* **197**, 803 (Mar 15, 2008).
41. S. Sridhar, K. A. Brokstad, R. J. Cox, Influenza Vaccination Strategies: Comparing Inactivated and Live Attenuated Influenza Vaccines. *Vaccines (Basel)* **3**, 373 (Apr 24, 2015).
42. M. R. Jenkins, R. Webby, P. C. Doherty, S. J. Turner, Addition of a prominent epitope affects influenza A virus-specific CD8+ T cell immunodominance hierarchies when antigen is limiting. *J Immunol* **177**, 2917 (Sep 1, 2006).
43. E. M. Anders, C. A. Hartley, P. C. Reading, R. A. Ezekowitz, Complement-dependent neutralization of influenza virus by a serum mannose-binding lectin. *J Gen Virol* **75 (Pt 3)**, 615 (Mar, 1994).

Acknowledgments: We thank Dr S Turner (Monash University, Australia) for the influenza viruses X31-OVA and PR8-OVA; and Dr N Zhang and M Bevan for TGFbRII KO OT-I mice. **Funding:** This work was supported by National Health and Medical Research Council of Australia. The Melbourne WHO Collaborating Centre for Reference and Research on Influenza is supported by the Australian Government Department of Health. **Author contributions:** A.P., P.R., and L.M.W designed the experiments. A.P., J.S., and L.M.W performed the experiments and data analysis. O.N and K.K. provided crucial experimental reagents. A.P., P.R., A.G.B and L.M.W contributed to writing the manuscript and editing of the manuscript. A.P., and L.M.W performed statistical analysis. **Competing interest:** The authors declare that they have no competing interests.

Figure 1: Memory $CD8^+$ T cells persist in the URT following influenza virus infection

(a) Groups of 5 C57Bl/6 mice receiving a TRT infection with 10^4 PFU of X31–OVA were killed 3 days later and titres of infectious virus were determined in clarified homogenates prepared from lung and nasal tissues by standard plaque assay. Symbols represent individual mice and horizontal bars represent the mean $\pm$ SEM of viral titres. (b) Mice injected with 10^4 naïve $CD45.1^+$ $CD8^+$ OT-I T cells and receiving a TRT infection with 10^4 PFU X31-OVA were killed 6 days later. Fluorescence microscopy (x 20 objective) was then performed to detect influenza virus nucleoprotein (NP) and CD3+ T cells in nasal tissues. (c) Mice injected with 10^4 naïve $CD45.1^+$ $CD8^+$ OT-I T and infected with 10^4 PFU of X31-OVA were killed at day 35. Representative flow cytometry plots of single cell suspensions from the lung and nasal tissue were gated on OT-I ($CD45.1^+$ $CD8^+$) cells and assessed for CD103 and CD69 expression (d) Mice injected with 10^4 naïve $CD45.1^+$ $CD8^+$ OT-I T cells prior to TRT infection with 10^4 PFU of X31-OVA received an intravenous injection of anti-CD8-PE (CD8-iv) at day 30 post-infection and were killed 5 min later for tissue harvest. For flow cytometry analysis, single cell suspensions from the spleen, lung, blood and nasal tissue were gated on OT-I ($CD45.1^+$ $CD8^+$) cells and assessed for CD103 expression and location ($CD8\text{-}iv^{lo}$: parenchyma associated cells; $CD8\text{-}iv^{hi}$: circulating cells) (e-f) Mice seeded with 10^4 naïve $CD45.1^+$ $CD8^+$ OT-I T cells and receiving TRT infection with 10^4 PFU of X31-OVA were administered CFSE intranasally 20 days later into the URT and the proportion of $CFSE^+$ $CD45.1^+$ $CD8^+$ OT-I T cells in the nasal tissue and spleen were measured 3, 20 and 40 days after CFSE delivery. (e) Data pooled from 3 independent experiments with the symbols representing individual mice and the bars representing mean $\pm$ SEM (n=5-7 mice per group; 1-way ANOVA, Tukey's multiple comparison). (f) Representative flow cytometry profiles showing expression of CFSE and CD103 on $CD45.1^+$ $CD8^+$ OT-I T cells. (g) Microscopy of the nasal tissue highlighting the NALTs, nasal turbinates, and nasal septum (DAPI). (h) Microscopy of NALTs from mice staining of B220, CD3, and DAPI are shown. (i) Mice injected with naïve $CD45.1^+$ $CD8^+$ OT-I T cells received a TRT infection with 10^4 PFU X31-OVA and were killed for analysis at day 30 p.i. Microscopy of the various area of nasal tissue staining for CD45.1+ (OT-I cells) and DAPI are shown. (j) Flow cytometry profiles depicting OT-I cells ($CD45.1^+CD8^+$) isolated from the NALTs and nasal tissue isolated from mice injected with naïve $CD45.1^+$ $CD8^+$ OT-I T cells received a TRT infection with 10^4 PFU X31-OVA and killed for analysis at day 30 p.i. (k)

Histograms represent the expression levels of CD103 on OT-I cells isolated from the NALTs or nasal tissue. Numbers represent mean MFI ± SEM (l) Absolute number of $CD103^+CD69^+$ OT-I T cells in the NALTs and nasal tissue of mice described in (j). Data pooled from 3 experiments, bars represent the mean ± SEM (n=8 mice per group; Mann Whitney test)

Figure 2. Tissue resident memory $CD8^+$ T cells develop in the URT following influenza infection independently of local antigen presentation and establishment of Trm is only partially dependent on TGFβ signaling.

(a) Expression of CD69 and CD103 on OT-I T cells in the lung and nasal tissue of mice seeded with 10^4 naïve $CD45.1^+$ $CD8^+$ OT-I T cells followed by TRT infection with 10^4 PFU of X31-OVA and analysed on day 30 post-infection. (b) Heat-map depicts relative expression of Trm signature genes in subsets of OT-I cells sorted from nose and lung (as indicated in a) and memory ($CD44^+$) $CD62L^+$ and $CD62L^-$ OT-I sorted from the spleen of mice that received 10^4 naive $CD45.1^+$ $CD8^+$ OT-I cells followed by TRT infection with 10^4 PFU of X31-OVA and assessed at 30 days p.i. Results are presented as expression relative to housekeeping and data are pooled from five experiments. (c-f) The absolute number of $CD45.1^+$ $CD8^+$ OT-I T cells in the (c) nose and (d) lung of mice seeded with either wild-type (WT) or *Tgfbr2*$^{f/f}$dLck-Cre (TGFβRII KO) naïve $CD45.1^+$ $CD8^+$ OT-I T cells, followed by TRT infection with 10^4 PFU of X31-OVA and analyzed at 6, 10, and 20 p.i. Data pooled from 3 experiments, bars represent the mean ± SEM (n=6-16 mice per group; 2-way ANOVA, Sidak's multiple comparison) (e-f) Absolute numbers of WT and TGFβRII KO $CD103^+$ $CD69^+$ Trm OT-I in the (e) lung and (f) nasal tissues of mice at day 10, 20 and day 60 p.i. Data pooled from 3 experiments, bars represent the mean ± SEM (n=6-19 mice per group; 2-way ANOVA, Sidak's multiple comparison) (g) Quantitative PCR analysis of the expression of various genes in $CD103^+CD69^+$ TGFβRII KO $CD45.1^+$ $CD8^+$ OT-I (KO) or $CD45.1^+$ $CD8^+$ OT-I (WT) T cells sorted from the nasal tissue of mice that received naïve TGFβRII KO $CD45.1^+$ $CD8^+$ OT-I or $CD45.1^+$ $CD8^+$ OT-I cells followed by TRT infection with 10^4 PFU of X31-OVA and assessed at day 20 p.i. Results are presented as expression relative to housekeeping. Data are pooled from 3 experiments, bars represent the mean ± SEM (Mann-Whitney test, $*P<0.01$) (h-i) Analysis of CD103 and CD69 expression on memory $CD45.1^+$ $CD8^+$ OT-I T cells in lung and nasal tissue isolated from naïve mice or mice receiving TRT infection with 10^4 PFU of X31 or X31-OVA, 'seeded' with *in vitro*–activated OT-

I T cells 2 days later and analyzed on day 20 p.i. (h) The percentage and (i) absolute number of $CD45.1^+$ $CD8^+$ OT-I cells expressing CD103 and CD69 in the lung and nasal tissue. Data pooled from 3 experiments, bars represent the mean ± SEM (n=6-8 mice per group; 1-way ANOVA, Tukey's multiple comparison)

Figure 3. Trm that develop in the URT persist with minimal decay and provide long term protection against influenza virus re-challenge

(a) Mice injected with 10^4 naïve $CD45.1^+$ $CD8^+$ OT-I T cells and receiving a TRT infection with 10^4 PFU X31-OVA were killed at various time points post-infection and the absolute numbers of $CD103^+CD69^+$ OT-I T cells (Trm) in the lung and nasal tissue were determined. Symbols represent individual mice and bars represent the mean $\pm$ SEM (n=6-29 mice per group, data pooled from 5 independent experiments, 2-way ANOVA, Sidak's multiple comparison) (b-c) Mice injected with 10^4 naïve $CD45.1^+$ $CD8^+$ OT-I T cells and receiving a TRT infection with 10^4 PFU X31-OVA were re-challenged 20 or 120 days later via a TRT infection with PR8-OVA and the viral titres in the (b) lung and (c) nasal tissue was determined 3 days later. Symbols represent individual mice. Data pooled from two experiments, bars represent the mean $\pm$ SEM (n=5-8 mice per group, One way ANOVA, Tukey's multiple comparison)

Figure 4: Different immunodominance hierarchies among influenza-specific Trm in the lung and nasal tissue

Absolute numbers of NP_{366}-, PA_{224}- and $PB1_{703}$- specific $CD8^+$ T cells in the spleen, lung and nasal tissue of mice receiving a TRT infection with 50 PFU PR8 was determined at days (a) 10 and (b) 60 p.i. Data pooled from 2 independent experiments, symbols represent the mean ± SEM (n=5-11 mice per group; 2-way ANOVA with Tukey's multiple comparison) (c-f) Expression of CD69 and CD103 on NP_{366}-, PA_{224}- and $PB1_{703}$- specific $CD8^+$ T cells in the lung and nasal tissue of mice receiving a TRT infection with 50 PFU of PR8 and analysed on day 60 p.i. The (d) percentage and (e-f) absolute number of CD103+CD69+ NP_{366}-, PA_{224}- and $PB1_{703}$- specific $CD8^+$ T cells in the (e) nasal tissue and (f) lung on day 60 p.i. are shown. Data pooled from 2 experiments, bars represent the mean ± SEM (n=11 mice per group; 2-way ANOVA with Sidak's multiple comparison).

Figure 5: Relative epitope abundance modulates the immunodominance hierarchy within the lung Trm pool

(a) Mice were injected via the i.p. route with 10^4 PFU of PR8 and 6 days later were inoculated via the intranasal route with BMDCs pulsed with NP_{366}- and PA_{224}-peptide or un-pulsed BMDCs in the presence of LPS. Then, 21 days after BMDC immunization mice were killed and the absolute number of NP_{366}- and PA_{224}- specific $CD8^+$ T cells in the (b) spleen, and the (c) proportion and (d) absolute number of CD103+CD69+ NP_{366}- and PA_{224}- specific $CD8^+$ T cells in the lung was determined. Data pooled from 2 experiments, bars represent the mean ± SEM (n=6 mice per group; 2-way ANOVA with Sidak's multiple comparison)

Figure 6. Influenza-specific Trm in the URT blocks pulmonary influenza virus infection.

Viral titres in (a) nasal tissue and (b) lungs of mice 5 days after URT infection or TRT infection with PR8. Data pooled from 2 independent experiments, symbols represent titres from individual mice and bars represent the mean ± SEM (n=5-6 mice per group; Student's *t*-test) (c) Flow cytometry analysis of CD103 and CD69 expression on NP- or PA-tetramer+ cells in lung and nasal tissue of mice receiving an URT or TRT infection with PR8 and analysed on day 30 p.i. (d-f) Mice injected i.p with PR8 (i.p. PR8) or receiving an URT or TRT infection with PR8 infection were killed and analysed on day 30 p.i. (d) The absolute number of $CD8^+$ NP- and PA-tetramer+ cells in the spleen and the absolute number of $CD8^+$ NP- and PA-tetramer+ $CD103^+CD69^+$ Trm in the (e) lung and (f) nasal tissue were determined. Data pooled from 2 independent experiments, bars represent mean $\pm$ SEM (n=9-18 per group, 1-way ANOVA followed by Sidak's Multiple Comparison test). (g-j) Mice generated as described (d-f) were challenged on day 30 p.i. with X31 via an URT infection and the viral titers in the (g,i) nasal tissues and (h,j) lung were determined 3 days (g-h) or 5 days (i-j) later. Data pooled from 2 independent experiments, symbols represent individual mice, bars represent mean ± SEM (n=8-10 per group, 1-way ANOVA followed by Sidak's multiple comparison)

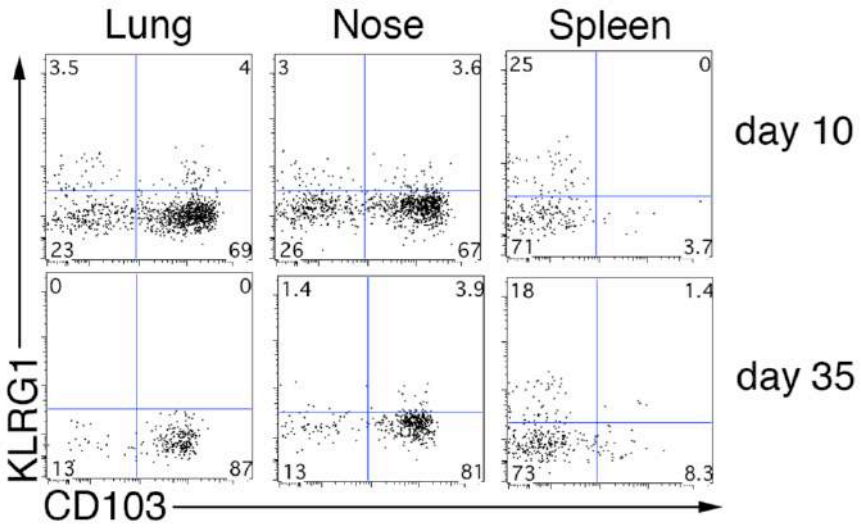

Figure S1. Lung and Nasal tissue Trm develop from KLRG1- precursor cells
Mice injected with 10^4 naïve CD45.1$^+$ CD8$^+$ OT-I T and infected with 10^4 PFU of X31-OVA were killed at day 10 and 35 p.i. Representative flow cytometry plots of single cell suspensions from the spleen, lung and nasal tissue were gated on OT-I (CD45.1$^+$ CD8$^+$) cells and assessed for CD103 and KLRG1 expression. Data representative of two independent experiments.

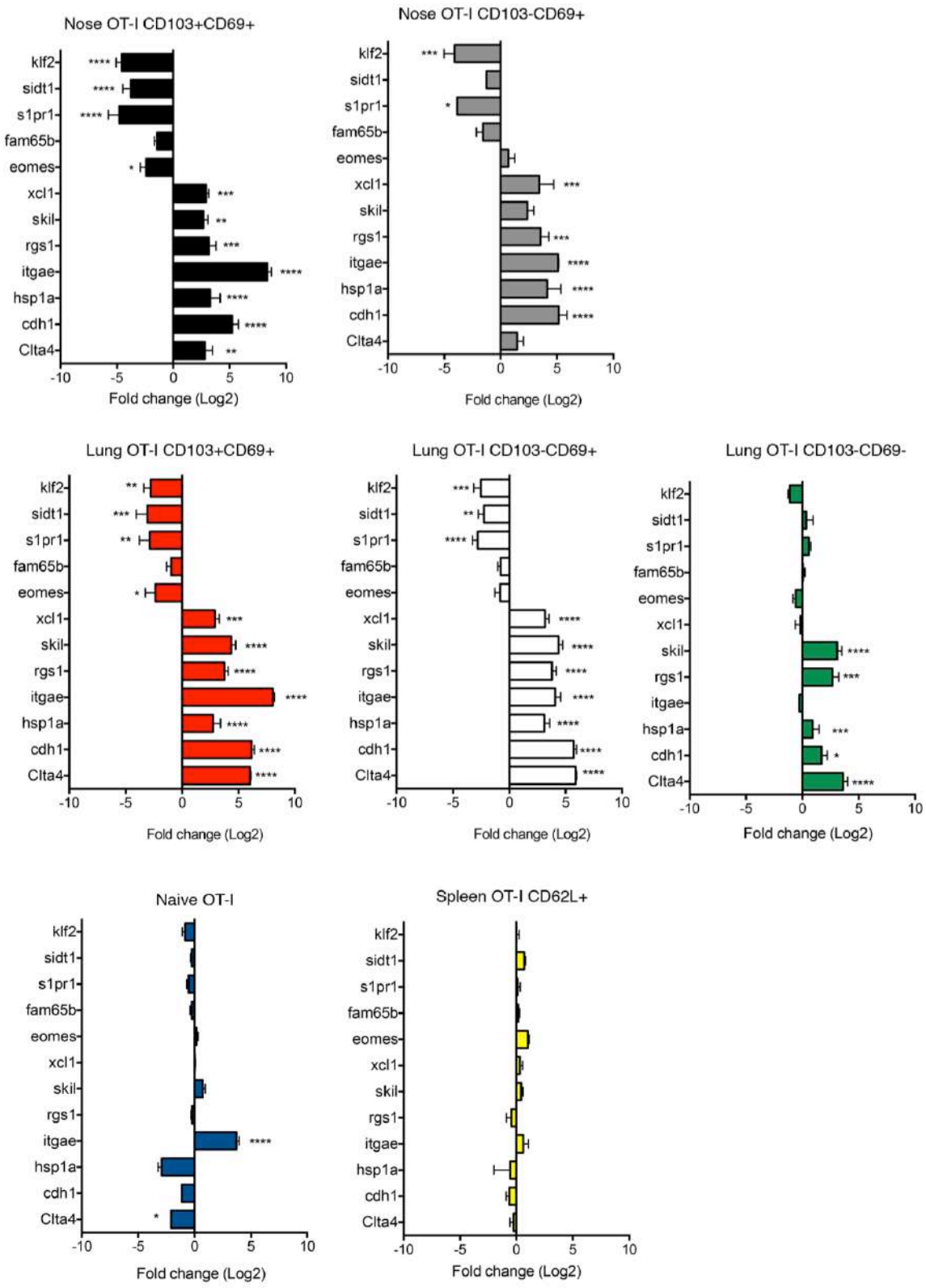

Figure S2. Molecular signature of nasal tissue Trm

Expression of Trm signature genes in subsets of OT-I cells sorted from nose and lung and memory ($CD44^+$) $CD62L^+$ and $CD62L^-$ OT-I sorted from the spleen of mice that received 10^4 naive $CD45.1^+$ $CD8^+$ OT-I cells followed by TRT infection with 10^4 PFU of X31-OVA and assessed at 30 days p.i. Results are normalized to 3 housekeeping genes. The log2-fold change in expression (relative to CD62L- effector memory T cells) for each Trm signature gene is displayed. Data are pooled from five experiments. 2-way ANOVA, Sidak's multiple comparison.

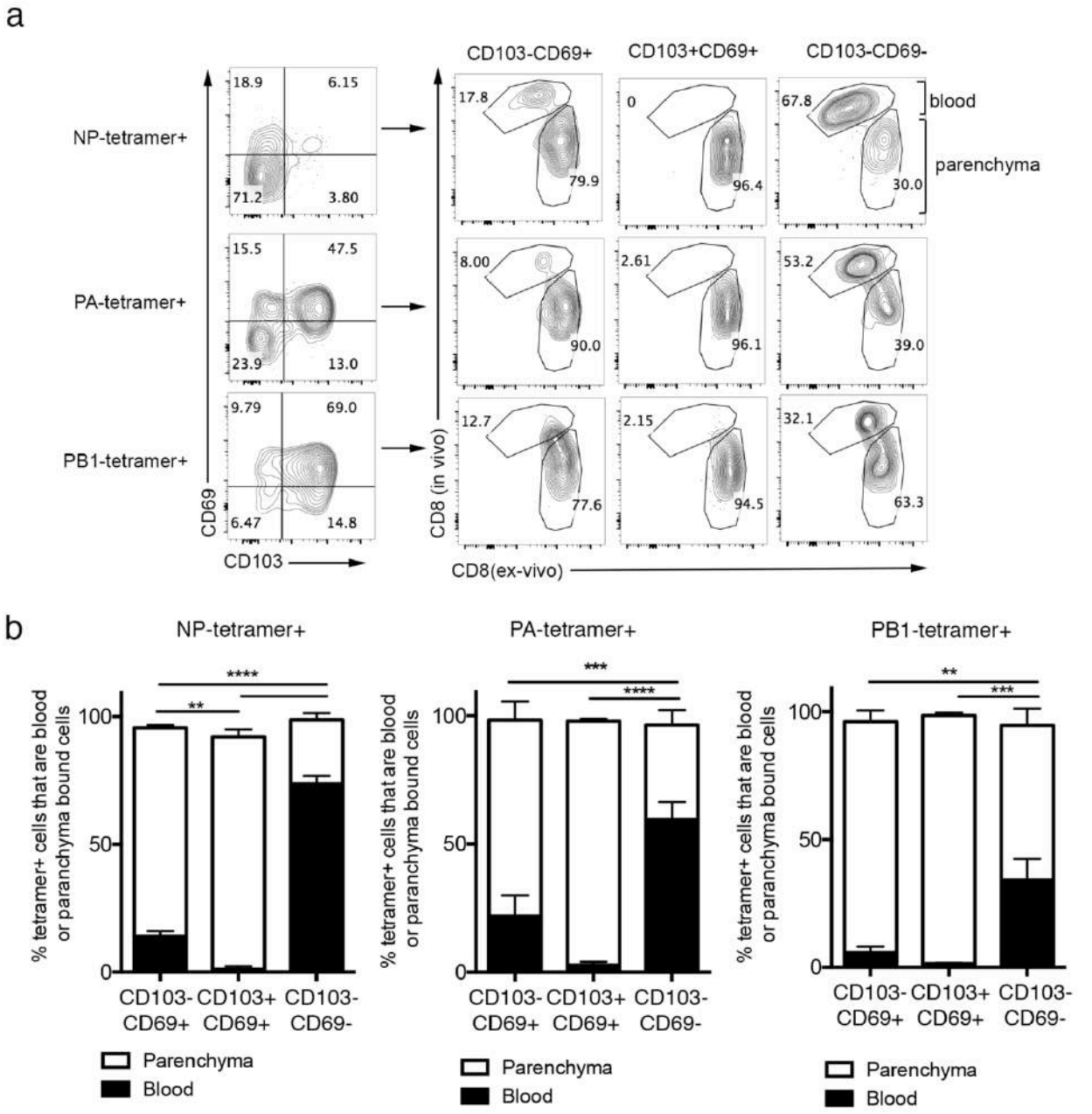

Figure S3. Localization of NP, PA and PB1 CD103+CD69+ Trm in the lung following influenza virus infection

Mice infected with 10^4 PFU of X31 received an intravenous injection of anti-CD8-PE (CD8-in vivo) at day 30 post-infection and were killed 5 min later for tissue harvest. (a) Flow cytometry analysis on single cell suspensions from lung gated on $PB1_{703}$-, PA_{224}-, NP_{366}-specific CD8+ T cells subsets and location (CD8-iv^{lo}: parenchyma associated cells; CD8-iv^{hi} : circulating cells) was determined. (b) Graphs depict the proportion of tetramer+ cells that are parenchyma or blood bound for each subset (data pooled from 2 experiments, n=4, 2-way ANOVA, Tukey's multiple comparison)

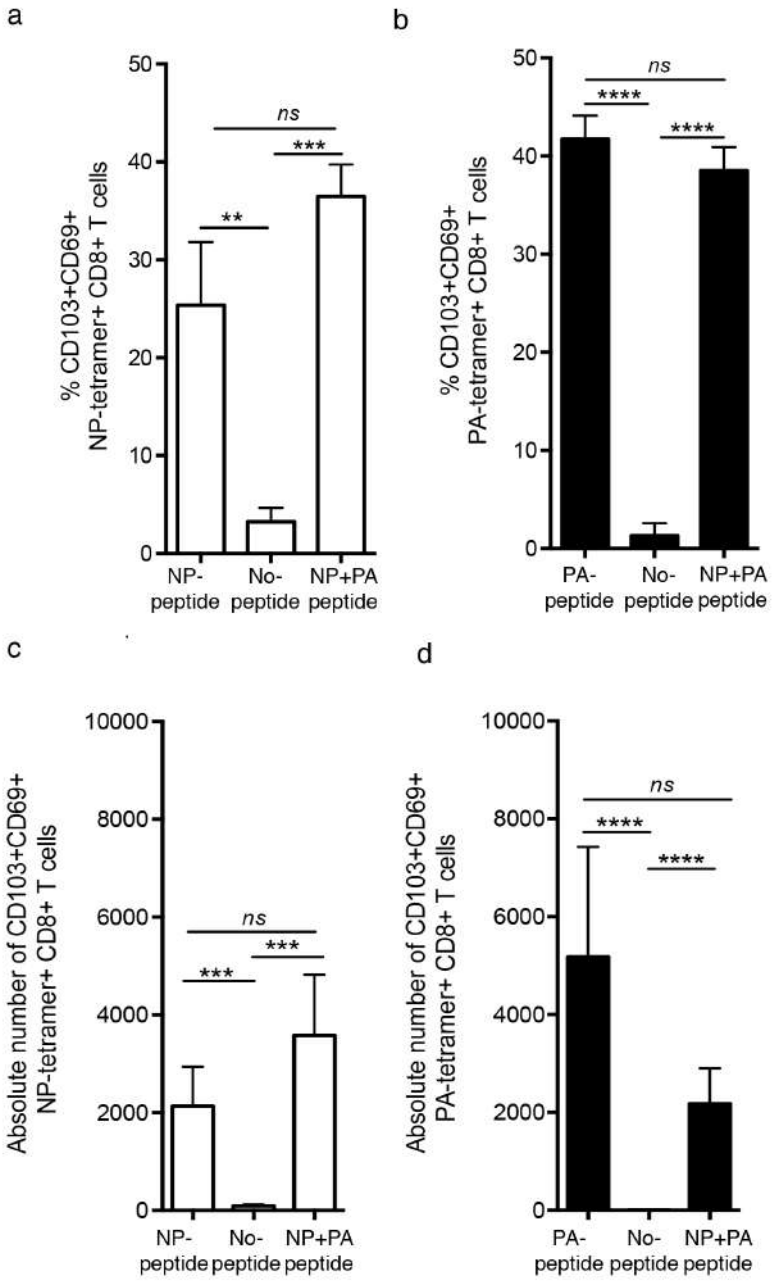

Figure S4: Trm development following DC immunization.
Mice were injected via the i.p. route with 10^4 PFU of PR8 and 6 days later were inoculated via the intranasal route with BMDCs pulsed with either NP_{366}- or PA_{224}- peptide, both or none. Then, 21 days after BMDC immunization mice were killed and the (a-b) proportion and (c-d) absolute number of CD103+CD69+ NP_{366}- and PA_{224}- specific $CD8^+$ T cells in the lung was determined. Data pooled from 2 experiments, bars represent the mean ± SEM (n=6 mice per group; 1-way ANOVA with Tukey's multiple comparison)

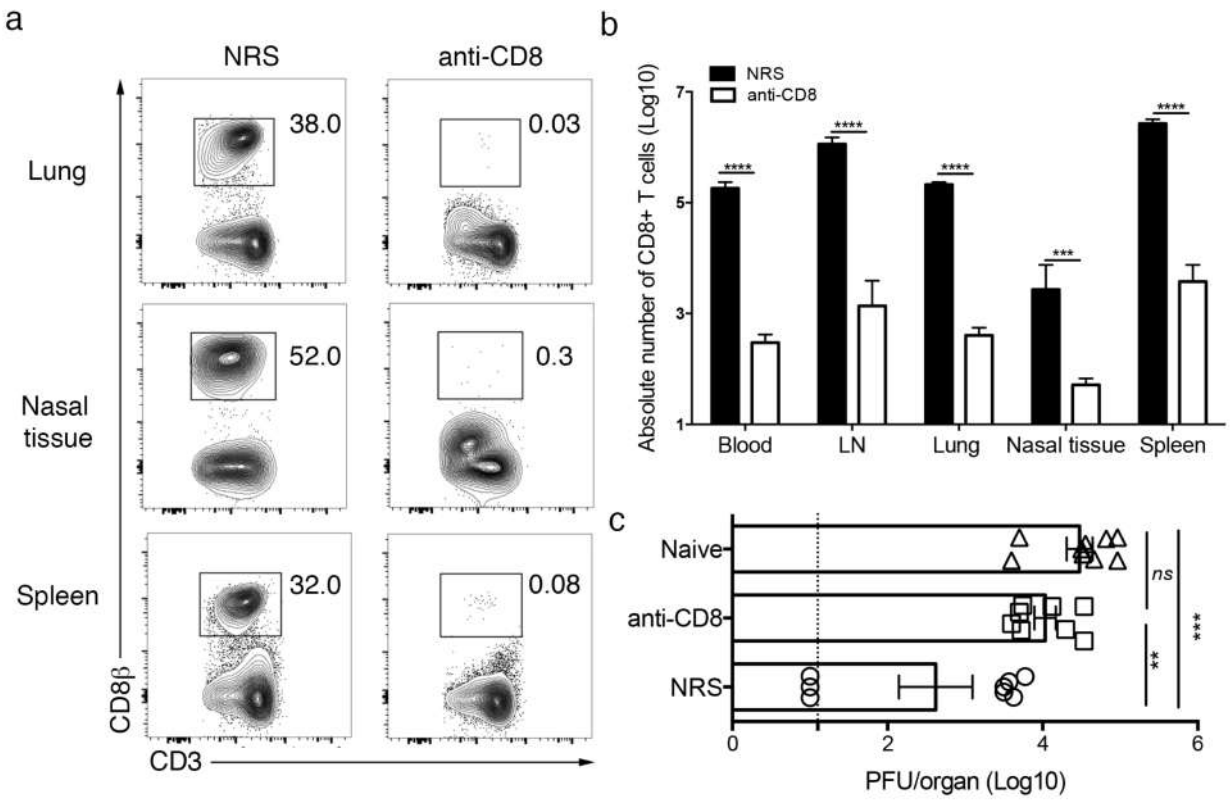

Figure S5: Depletion of CD8 T cells eliminates local protection in the nasal tissue following influenza virus re-- challenge.

(a) Mice infected with 50 PFU PR8 virus and on day 28 p.i were administered either normal rat serum (NRS) or anti-CD8 depletion antibody (clone 2.43) for 3 consecutive days. Representative flow cytometry profiles gated on CD3+ T cells and staining for CD8b in the lung, nasal tissue and spleen was measured on day 3 post treatment. (b) Absolute number of CD8+ T cells in the spleen, lung, Blood, LN and nasal tissue of control and CD8 depleted mice. Data pooled from 3 experiments (n=3, 2-way ANOVA, Sidak's multiple comparison). (c) Mice generated as described in (a) were re-challenged in URT with X31 and viral titres in the nasal tissue was determined on day 3 post infection. Data pooled from 2 experiments (n=8-9, 1-way ANOVA, Sidak's multiple comparison)

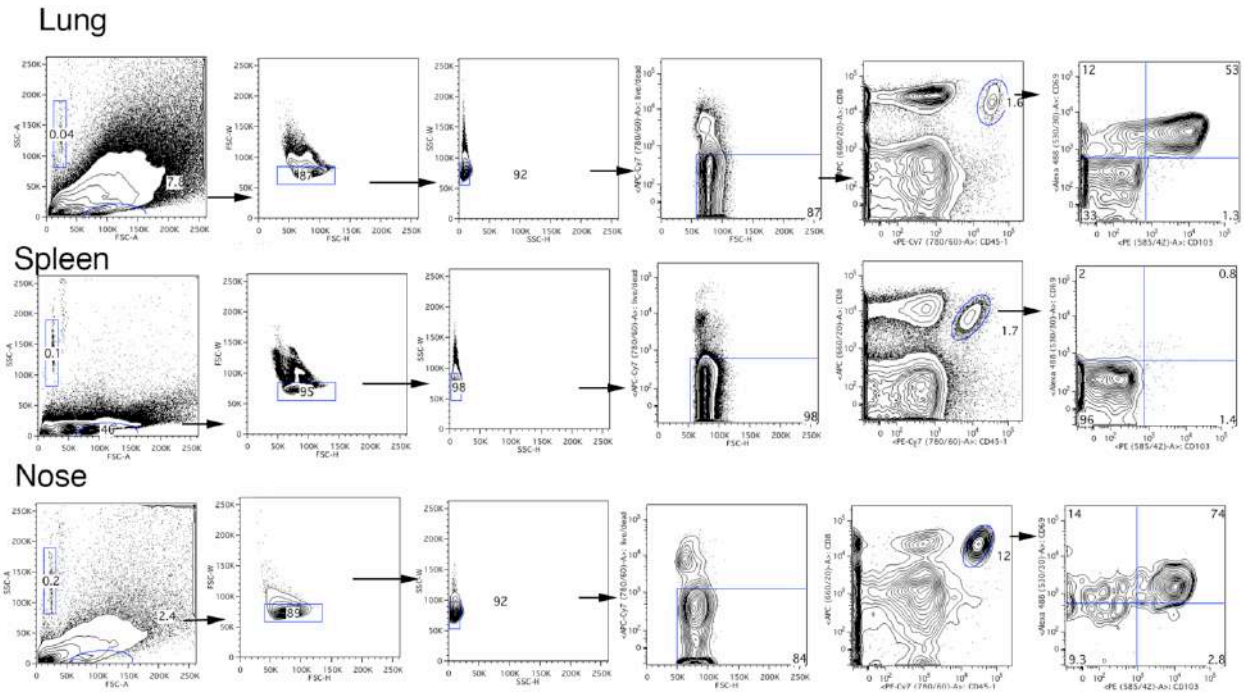

Figure S6: Gating strategy for identifying transgenic OT-- I in spleen, lung and nasal tissue of influenza virus infected mice.
Mice seeded with 10^4 naïve CD8+ CD45.1+ OT−I T cells prior to intranasal infection with influenza virus. Representative flow cytometry profiles are from mice harvested at day 30 p.i.

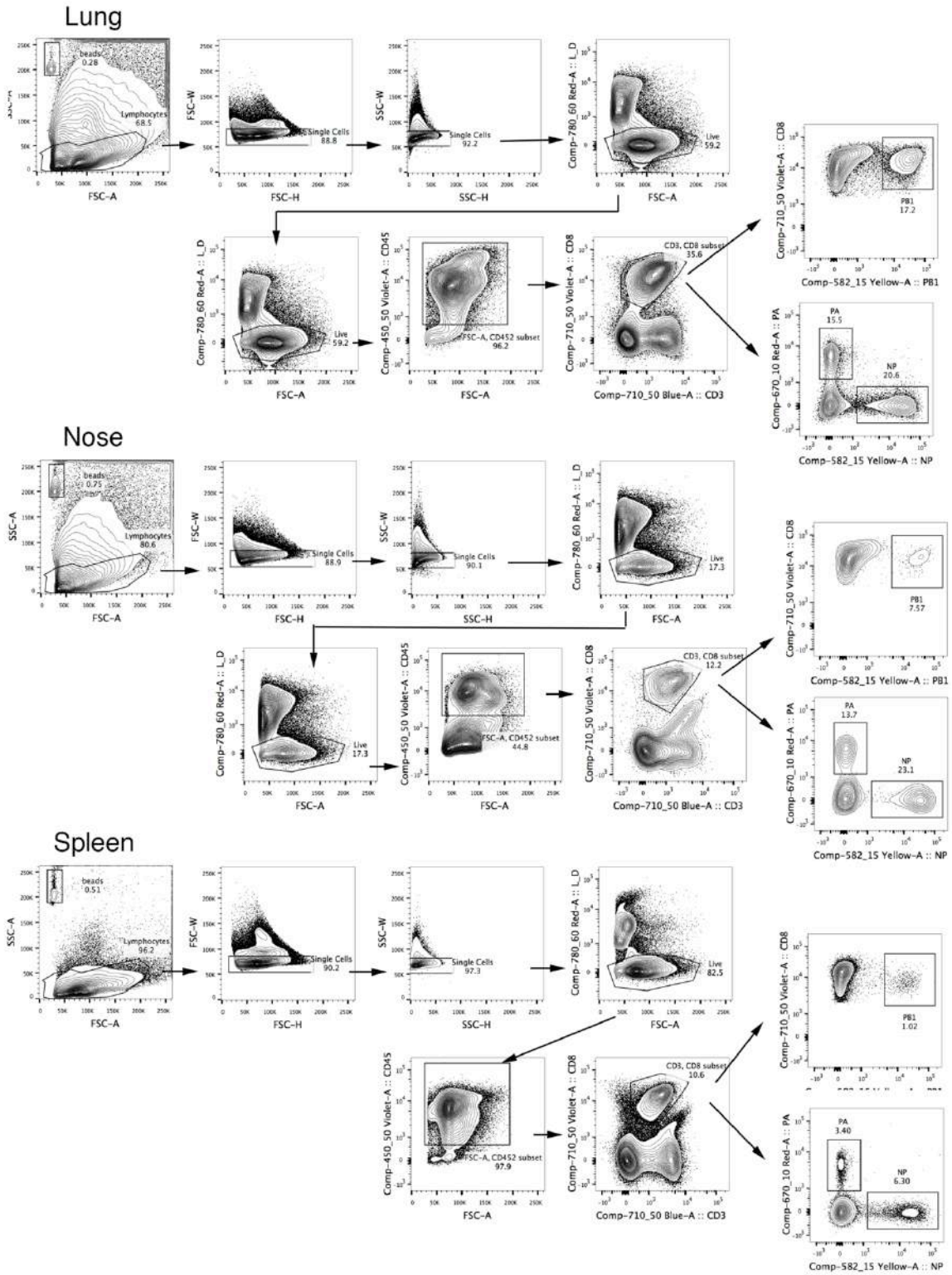

Figure S7: Gating strategy for identifying endogenous influenza virus specific CD8+ T cells in spleen, lung and nasal tissue of influenza virus infected mice.

Mice infected intranasally with influenza virus. Representative flow cytometry profiles are from mice harvested at day 10 p.i.

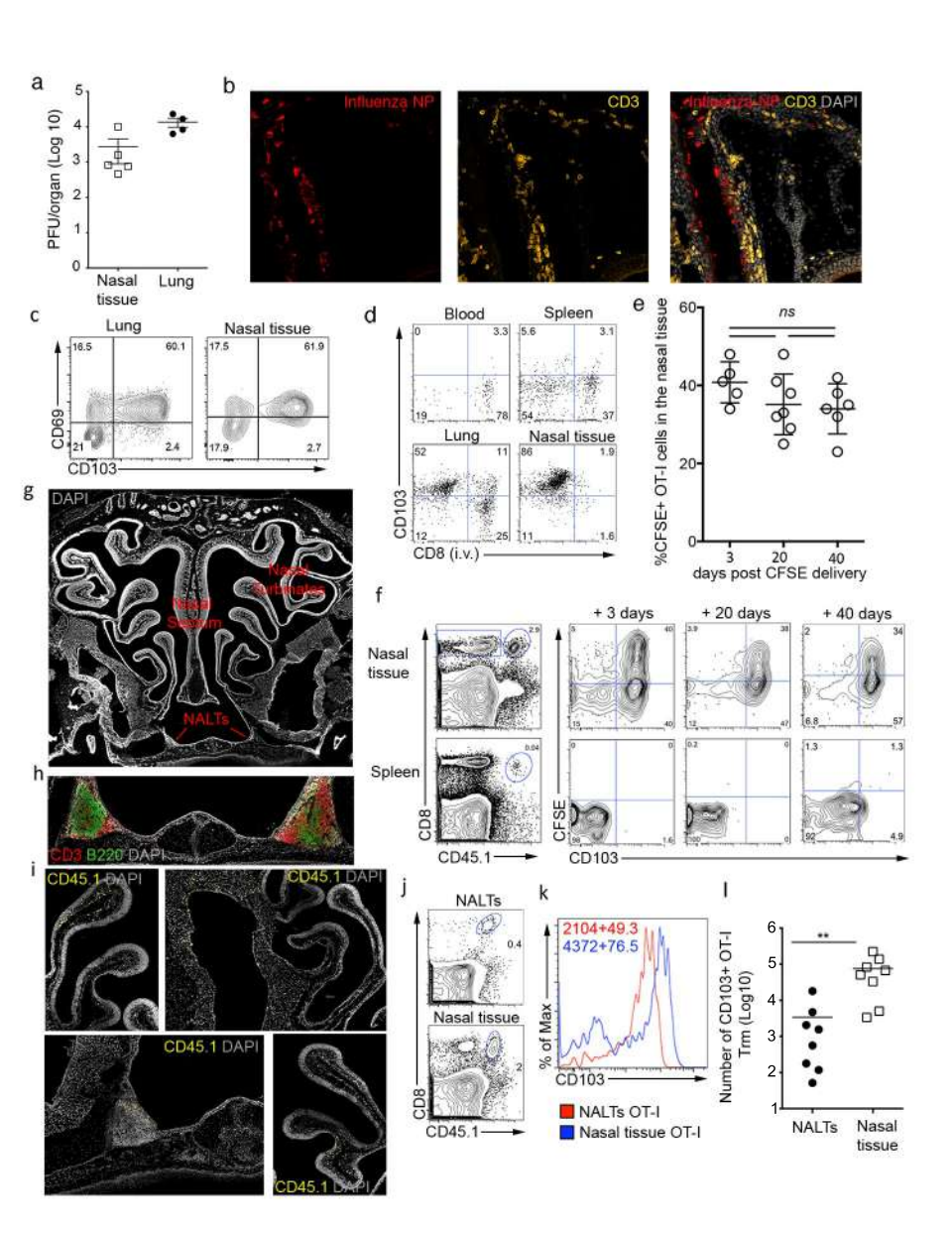
a
PFU/organ (Log 10)
Nasal tissue
Lung
b
Influenza NP
CD3
Influenza NP CD3 DAPI
c
Lung
Nasal tissue
CD69
CD103
d
Blood
Spleen
Lung
Nasal tissue
CD103
CD8 (i.v.)
e
ns
%CFSE+ OT-I cells in the nasal tissue
days post CFSE delivery
f
+ 3 days
+ 20 days
+ 40 days
Nasal tissue
Spleen
CD8
CFSE
CD45.1
CD103
g
DAPI
Nasal turbinates
Nasal Septum
NALTs
h
CD3 B220 DAPI
i
CD45.1 DAPI
j
NALTs
Nasal tissue
CD8
CD45.1
k
2104+49.3
4372+76.5
% of Max
CD103
NALTs OT-I
Nasal tissue OT-I
l
Number of CD103+ OT-I Trm (Log10)
NALTs
Nasal tissue

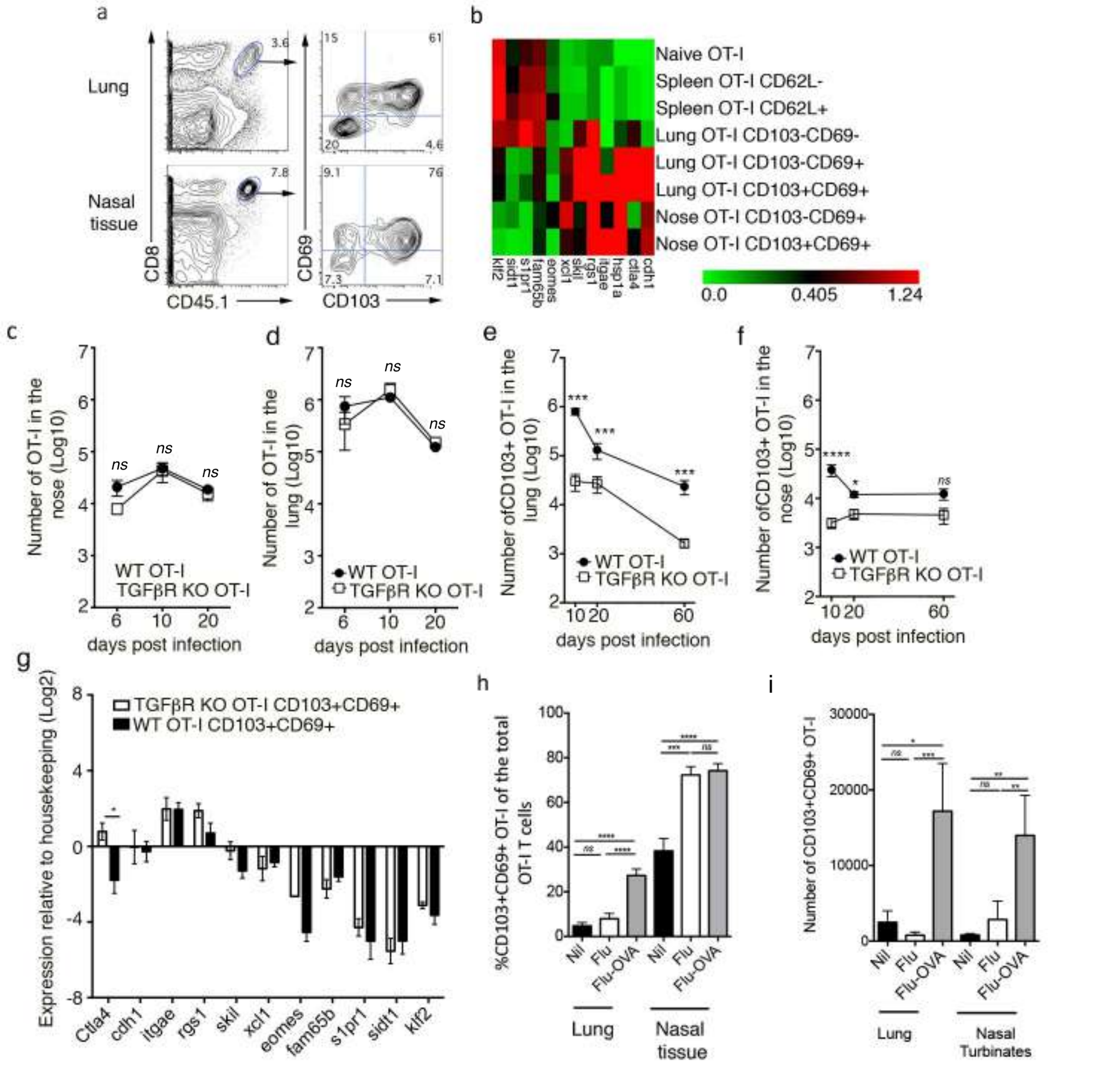
a
Lung
Nasal tissue
CD8
CD45.1
CD69
CD103
3.6
15
61
20
4.6
7.8
9.1
76
7.3
7.1
b
Naive OT-I
Spleen OT-I CD62L-
Spleen OT-I CD62L+
Lung OT-I CD103-CD69-
Lung OT-I CD103-CD69+
Lung OT-I CD103+CD69+
Nose OT-I CD103-CD69+
Nose OT-I CD103+CD69+
klf2
sipt1
s1pr1
fam65b
eomes
xcl1
skil
rgs1
itgae
hsp1a
ctla4
cdh1
0.0
0.405
1.24
c
Number of OT-I in the nose (Log10)
ns
WT OT-I
TGFβR KO OT-I
days post infection
d
Number of OT-I in the lung (Log10)
e
Number ofCD103+ OT-I in the lung (Log10)
***
f
Number ofCD103+ OT-I in the nose (Log10)
****
*
g
Expression relative to housekeeping (Log2)
TGFβR KO OT-I CD103+CD69+
WT OT-I CD103+CD69+
Ctla4
cdh1
itgae
rgs1
skil
xcl1
eomes
fam65b
s1pr1
sidt1
klf2
h
%CD103+CD69+ OT-I of the total OT-I T cells
Nil
Flu
Flu-OVA
Lung
Nasal tissue
i
Number of CD103+CD69+ OT-I
Nasal Turbinates

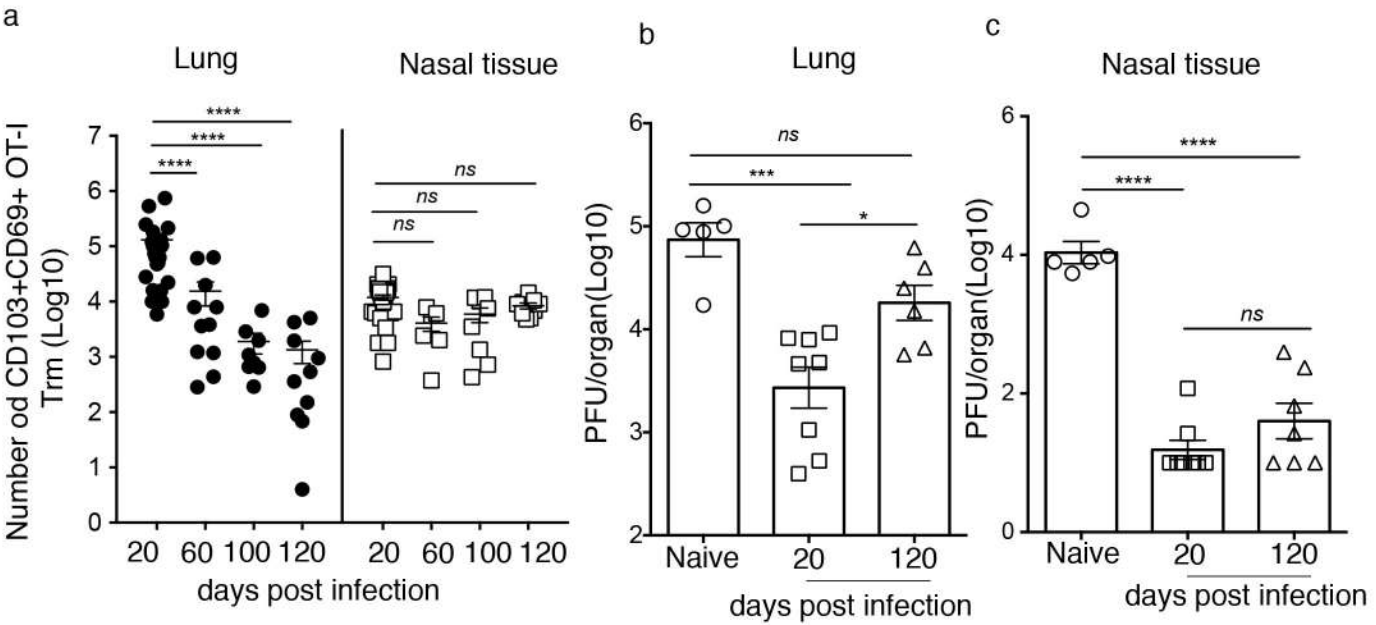
a
Lung
Nasal tissue
Number od CD103+CD69+ OT-I Trm (Log10)
****
****
****
ns
ns
ns
0
1
2
3
4
5
6
7
20 60 100 120 20 60 100 120
days post infection
b
Lung
PFU/organ(Log10)
ns
***
*
2
3
4
5
6
Naive 20 120
days post infection
c
Nasal tissue
PFU/organ(Log10)
****
****
ns
0
2
4
6
Naive 20 120
days post infection

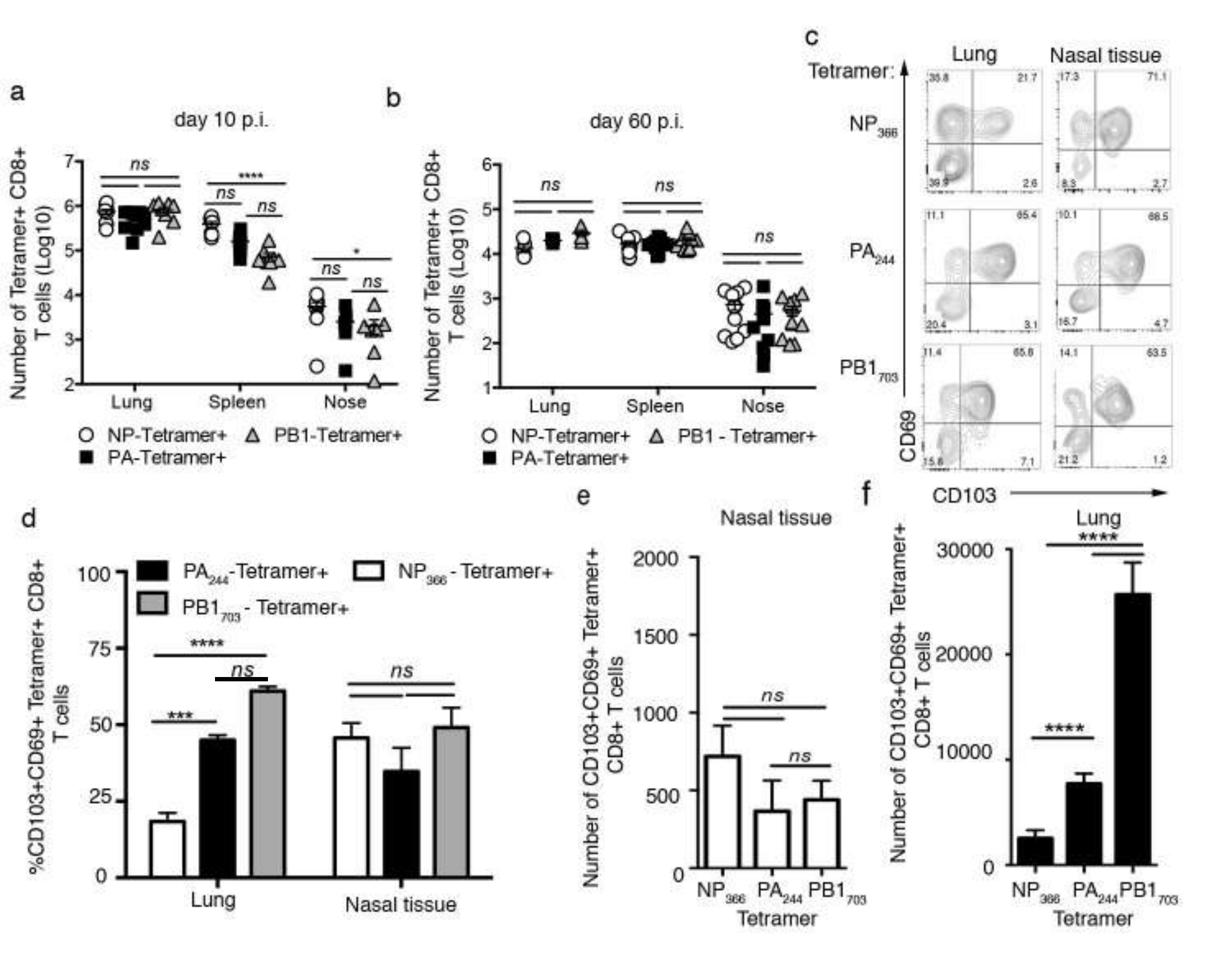
a
day 10 p.i.
Number of Tetramer+ CD8+ T cells (Log10)
Lung
Spleen
Nose
ns
****
*
NP-Tetramer+
PB1-Tetramer+
PA-Tetramer+
b
day 60 p.i.
Number of Tetramer+ CD8+ T cells (Log10)
Lung
Spleen
Nose
ns
NP-Tetramer+
PB1 - Tetramer+
PA-Tetramer+
c
Lung
Nasal tissue
Tetramer:
NP366
PA244
PB1703
CD69
CD103
d
PA244-Tetramer+
NP366 - Tetramer+
PB1703 - Tetramer+
%CD103+CD69+ Tetramer+ CD8+ T cells
***
****
ns
Lung
Nasal tissue
e
Nasal tissue
Number of CD103+CD69+ Tetramer+ CD8+ T cells
ns
NP366
PA244
PB1703
Tetramer
f
Lung
Number of CD103+CD69+ Tetramer+ CD8+ T cells
****
NP366
PA244
PB1703
Tetramer

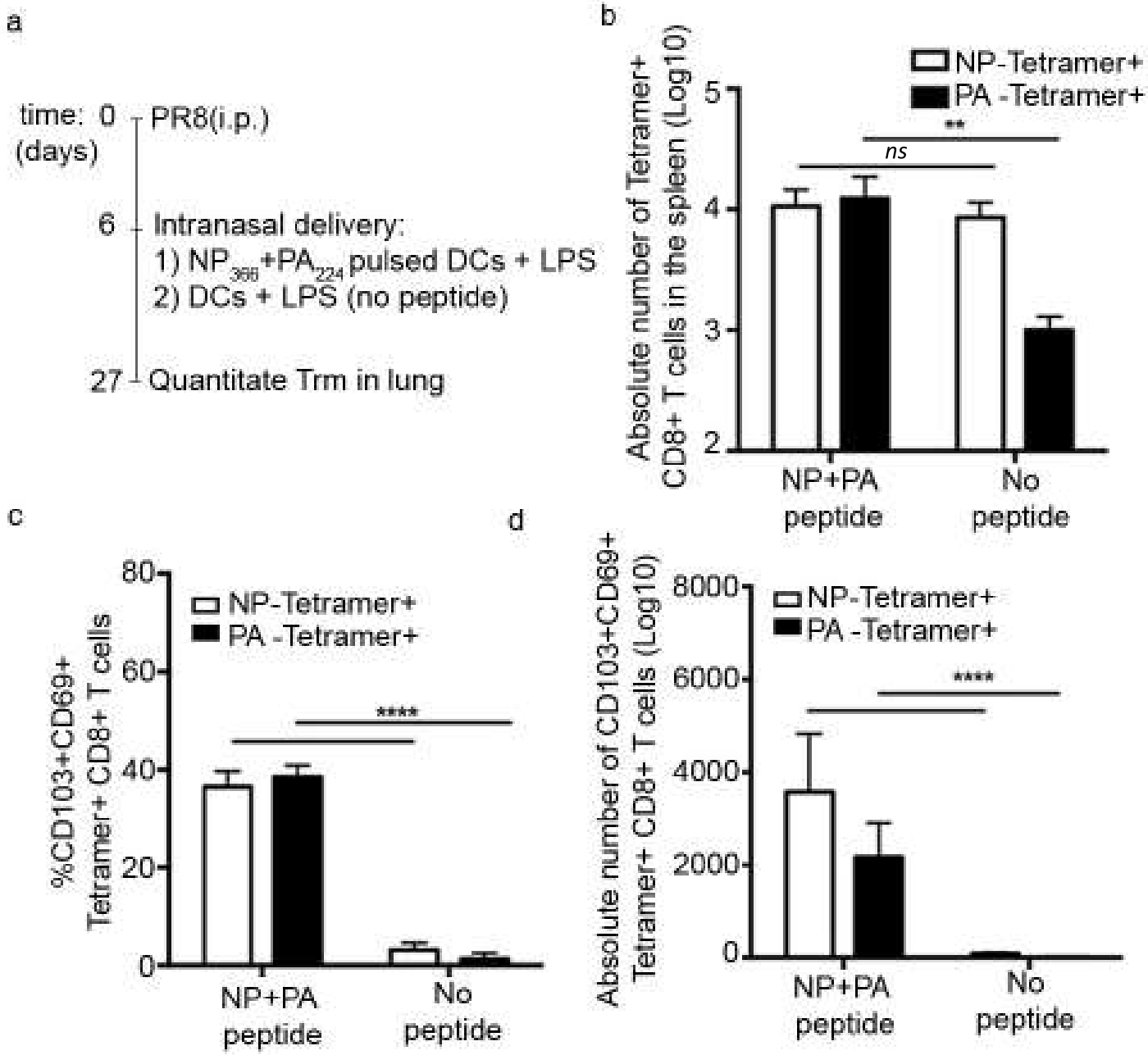
a
time: 0
(days)
PR8(i.p.)
6
Intranasal delivery:
1) NP366+PA224 pulsed DCs + LPS
2) DCs + LPS (no peptide)
27
Quantitate Trm in lung
b
NP-Tetramer+
PA -Tetramer+
**
ns
Absolute number of Tetramer+ CD8+ T cells in the spleen (Log10)
5
4
3
2
NP+PA peptide
No peptide
c
%CD103+CD69+ Tetramer+ CD8+ T cells
80
60
40
20
0
NP-Tetramer+
PA -Tetramer+
****
NP+PA peptide
No peptide
d
Absolute number of CD103+CD69+ Tetramer+ CD8+ T cells (Log10)
8000
6000
4000
2000
0
NP-Tetramer+
PA -Tetramer+
****
NP+PA peptide
No peptide

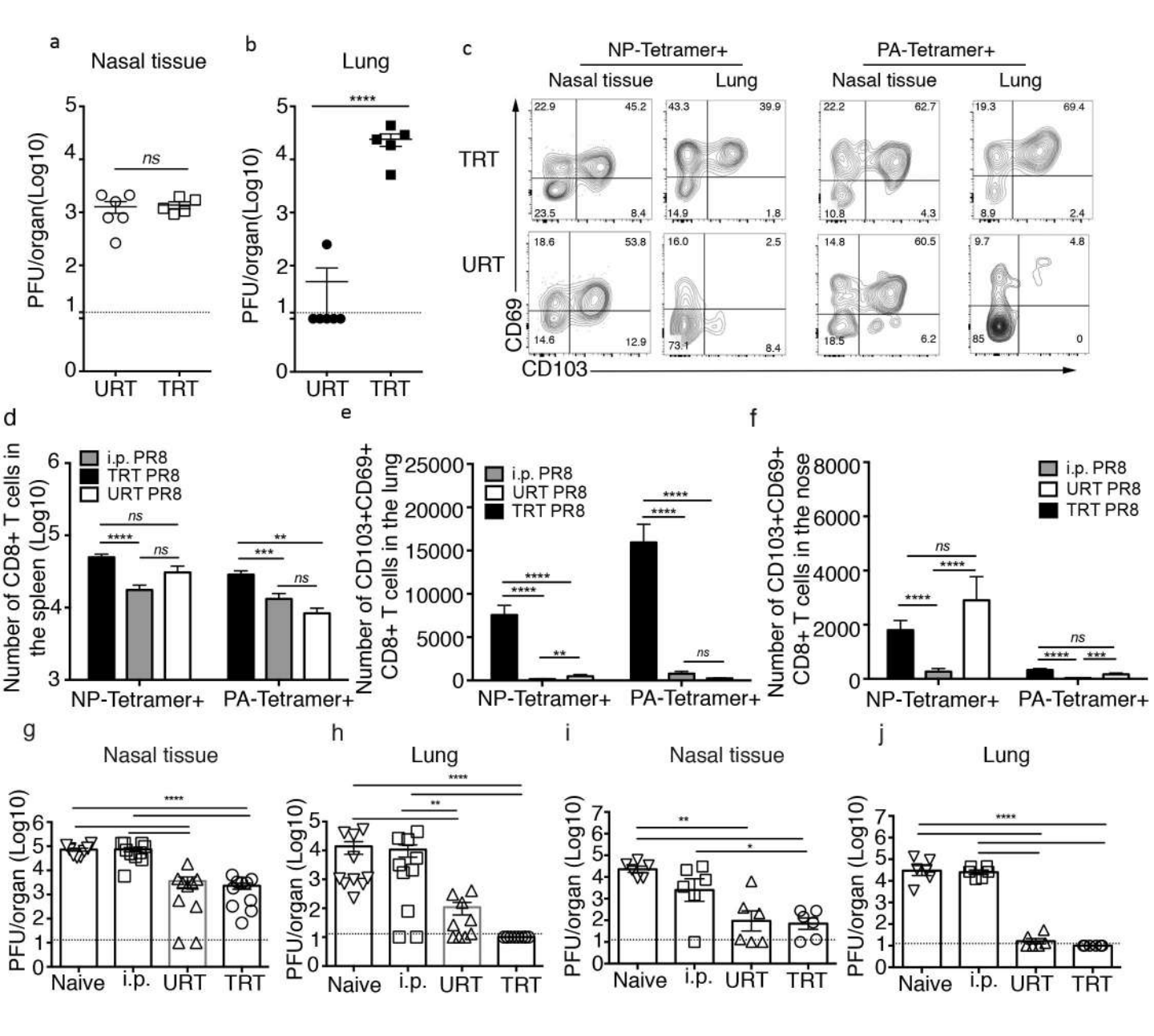
a
Nasal tissue
PFU/organ(Log10)
ns
URT
TRT
b
Lung
****
c
NP-Tetramer+
PA-Tetramer+
Nasal tissue
Lung
TRT
URT
CD69
CD103
d
Number of CD8+ T cells in the spleen (Log10)
i.p. PR8
TRT PR8
URT PR8
e
Number of CD103+CD69+ CD8+ T cells in the lung
f
Number of CD103+CD69+ CD8+ T cells in the nose
g
h
i
j
Naive
i.p.